COMMERCIAL – IN – CONFIDENCE

NATIONAL INSTITUTE FOR APPLIED
STATISTICS RESEARCH AUSTRALIA
University of Wollongong
NSW 2522
AUSTRALIA
Tel.: +61 2 4221.5435
Fax: +61 2 4221 4845
https://niasra.uow.edu.au/index.html

NIASRA
NATIONAL INSTITUTE FOR APPLIED STATISTICS RESEARCH AUSTRALIA

2014 OMAN RAIN ENHANCEMENT TRIAL
FINAL REPORT

TRADING & INVESTMENT ESTABLISHMENT

Australian Rain Technologies

February 2015

Copyright, Disclaimer and Acknowledgements

Prepared by:

Dr. Stephen Beare
National Institute For Applied Statistics Research Australia
University of Wollongong
NSW 2522
AUSTRALIA

Prof. Ray Chambers
National Institute For Applied Statistics Research Australia
University of Wollongong
NSW 2522
AUSTRALIA

Mr. Scott Peak
Australian Rain Technologies
Pier 8/9, 23 Hickson Rd, Millers Point
NSW 2000
AUSTRALIA

Document Control Information

Revision	Date	Description
1	14 Feb 15	Initial issue

This document contains the following pages, which are at the same issue as the latest issue shown in the table above.

Description	Number of Pages
Cover	1
Preliminary Pages	4
Main Section	61
Appendix A	4
Total	70

CONTENTS

EXECUTIVE SUMMARY

Oman is located in what is arguably the most water-stressed region in the world, faced with increasing water demand and diminishing fresh groundwater reserves. A technology that has the potential to increase natural rainfall and availability of water resources is of major interest. The challenge is to establish the efficacy and reliability of the technology in an operating environment that is characterised by highly variable patterns of natural rainfall.

A rainfall enhancement trial using the ATLANT™ ground-based ionisation technology was conducted in the Hajar Mountains from May to October in 2013. Data for the trial were obtained from 120 rain gauges, 13 automatic weather stations and upper air sounding at Seeb airport. The trial employed a randomised crossover design with two ion emitters (designated H1 and H2).

Randomised experimental designs can offer a limited degree of control over meteorological conditions and eliminate experimental bias. A model-based statistical analysis of the trial data was carried out to further control for the natural spatial and temporal variation in rainfall to better identify an enhancement signal should it exist.

The methodology used was initially developed for the ATLANT™ trials conducted in Australia, and is based on dynamic downwind target and control areas defined by daily wind directions and speeds. Meteorological and spatial covariates are then introduced in order to predict gauge level rainfall, allowing a comparison of observed rainfall in a target area with an estimate of the rainfall that would have occurred under natural conditions.

The model specification used for this purpose had a number of features to limit the potential bias in its predictions; including the use of an instrumental variable to predict naturally occurring downwind rainfall, as well as day and gauge-level random effects. While gauge-level analysis offers considerable gains in efficiency over the analysis of average rainfall readings in the target and control areas, correlation between rainfall measurements from gauges that are nearby, in both space and time, can lead to overstatement of the precision of measurement of natural rainfall levels and any consequent enhancement effects. A spatiotemporal bootstrap procedure was developed to account for this correlation, and this leads to a more accurate estimate of the precision of the model estimates of these quantities.

There are substantive differences in meteorology and topography of the trial areas in Australia and Oman, and two different downwind footprint models were evaluated in the 2013 trial, the downwind arc or wedge model used in the Australian trials was compared with a corridor model that bisected the area between the active and control site, substantially eliminating the overlap in the target and control gauge designations.

Overall, a positive and significant rainfall enhancement effect attributable to the operation of the emitters was observed (18.0 per cent at a confidence level of 99 per cent). This was supported in the 2014 trial with two additional ATLANT™ sites, an expanded and more targeted gauge network and additional instrumentation. In particular, two SODAR vertical wind profilers were installed to measure horizontal wind speed and direction and vertical wind speed above the H1 and H2 ATLANT™ sites .

The 2014 trial also employed a randomised crossover design, in this case applied to two pairings of two ATLANT™ sites. Four statistical models were used to identify and measure whether the ATLANT™ systems generated a rainfall enhancement signal during the trial. These included a 'corridor' and a 'wedge' model using data from H1 and H2, intended to provide estimates that are comparable to the data and methodology used in 2013, as well as

a ‘corridor’ model using data from all four ATLANT™s, and a ‘corridor’ model using data from H1 and H2 combined from the 2013 and 2014 trials.

All of the models generated significant ATLANT™ attributions (rainfall enhancement effect) with estimates very similar to 2013. The data for the full 2014 trial gave a very large estimate of the enhancement effect, however there are reasons to be circumspect about this result. The estimates obtained by combining H1 and H2 data from 2013 and 2014 provided perhaps the most reliable ATLANT™ attribution results to date. This combined data set yielded an enhancement effect of 18.5 per cent and a confidence level of 99 per cent.

The expanded gauge network provided a much better picture of the temporal and spatial viability of rainfall in the Hajar Mountains and appears to have increased the reliability of the estimates at H1 and H2, in the centre of the trial area. The continued expansion of the network should prove valuable. The addition of SODAR at H1 and H2 provided a better understanding of the orographic features of the trial area and informed the choice of the downwind footprint that is critical to the statistical analysis of the trials. The most significant improvement in future instrumentation would be an afternoon Seeb radiosonde to track the flow of upper winds during the time convective clouds form over the Hajar Mountains.

1. INTRODUCTION AND STRUCTURE OF THE REPORT

1.1. Background

The Sultanate of Oman is characterized by limited resources of freshwater, in combination with extremely high summer temperatures and high evaporation rates. During the last three decades the country witnessed spectacular socio-economic developments stimulated by oil exploration and production. This expansion and urbanisation has intensified the pressure on Oman's limited water resources (Charabi and Al-Hatrushi, 2009), resulting in Oman becoming one of most water-stressed countries in the world, highly dependent on declining groundwater resources (FAO, 2009). Hence a technology that has the potential to increase rainfall or mitigate projected future reduced rainfall is of considerable interest. The challenge is to establish the efficacy and reliability of the technology in an operating environment that is characterised by highly variable patterns of natural rainfall.

1.2. Previous trials – Oman 2013

Trading and Investment Establishment (TIE) contracted Australian Rain Technologies (ART) for the operation of a rainfall enhancement trial using the ATLANT™ technology in the Hajar Mountains in 2013. The trial was managed from a local TIE project headquarters in Oman including the coordination of the operations of the ATLANT™ sites and installation of new data instrument arrays across the trial region. The 2013 Oman Rainfall Enhancement Trial was built on the series of ATLANT™ trials undertaken in Australia 2007-2010 (Beare et al. 2010; 2011; Chambers et al. 2012).

1.2.1. Location and timing of 2013 trial

In 2013, two ATLANT™ locations were be used to target the Batinah/Dakhliyah Region of Oman (Figure 1-1). This region was chosen considering synoptic and local wind flows, cloud types, widespread uplift, and moisture availability. Such features affect the delivery of charged particles or aerosols to the cloud layer and potential subsequent rainfall enhancement. In addition, this period was chosen to capture the reported high incidence of convective storms over the Hajar Mountains with consistently suitable microphysical conditions for rainfall enhancement operations and where irrigation flow and ground water recharge occurs. In Oman, groundwater recharge is found to be most prominent in the Wadis (dry river beds) that cut through the mountains.

The trial operation ran for 170 days from 15 May to 31 October 2013. The trial area included 120 rain gauges and two automatic weather stations installed by TIE, as well as weather stations and upper soundings at Seeb international airport provided by the Oman Directorate General of Meteorology and Air Navigation (DGMAN). The trial results have been submitted for publication (Chambers et al. 2015).

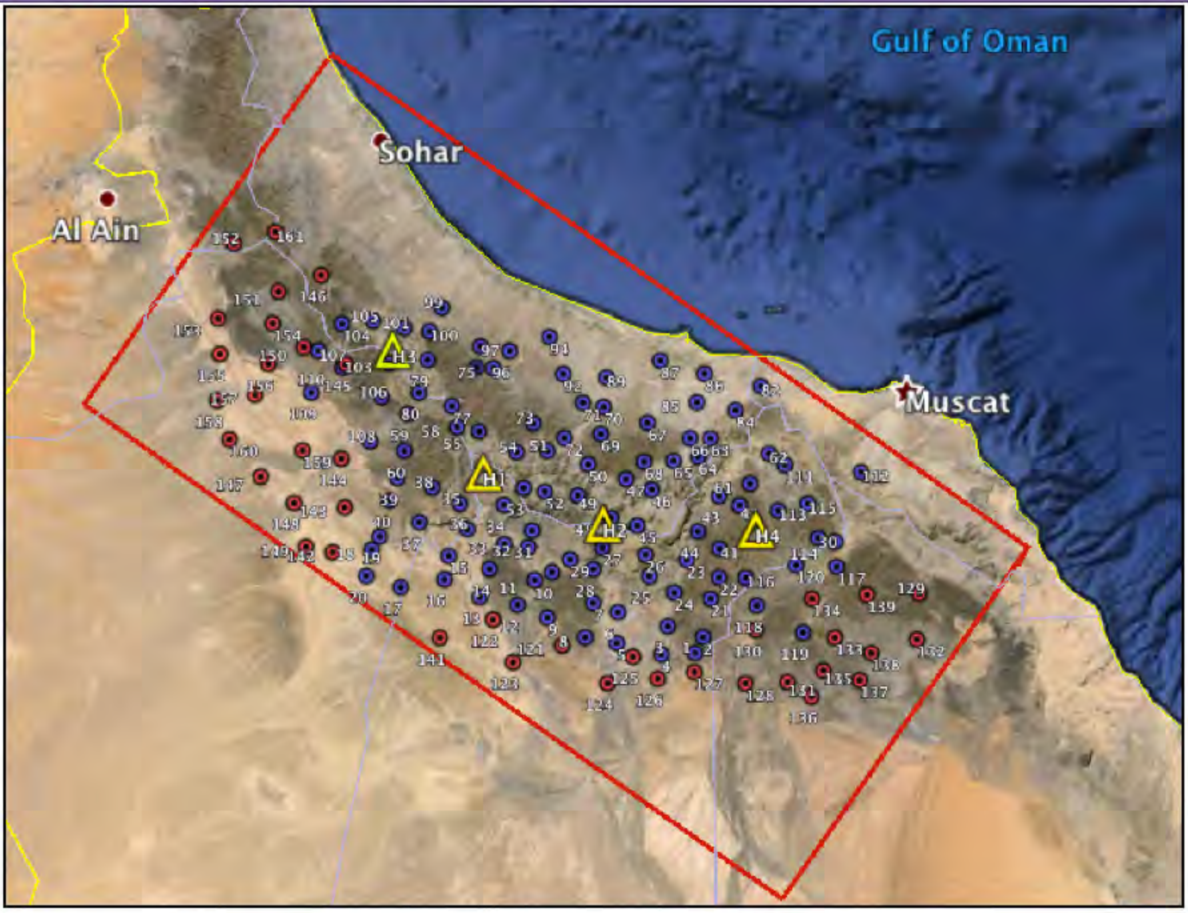

Figure 1-1 Trial Gauges (red dots), ATLANT™ Sites (yellow triangles) (right)

1.2.2. Experimental design and evaluation of trial data

Independent assessment of the 2013 trial was conducted by the National Institute for Applied Statistics Research Australia (NIASRA), at the University of Wollongong, to determine any effect attributable to the ATLANT™ technology. The analysis was based on rainfall and meteorological measurements recorded during the trial, using robust statistical analysis methods. The trial employed a randomised crossover design with the two ATLANT™s operated in a pre-determined randomised alternating schedule and a nominal switching time at 7am (local Oman time) on the designated days. Statistical spatio-temporal modelling was used to analyse the trial data. The aim of the modelling is to reduce the natural rainfall variation by using covariates to predict or explain the natural variation independently of the rainfall itself, facilitating the prediction of the level of rainfall that would have occurred if the ATLANT™ system were not operating.

The methodology was developed for weather modification trials in Australia based on defining the ATLANT™ 'footprint' dynamically in terms of target and control areas corresponding to two overlapping 60° arcs (or 'wedges') emanating from each of the ATLANT™ sites and oriented downwind in the direction of the steering wind. However, given that there are substantive differences in the prevailing weather conditions at the two ATLANT™ sites in the 2013 Oman trial and that the available meteorological data about the behaviour of steering winds over the course of a day is limited, it was decided that this was not the most robust model for defining a footprint in the Oman trial. A simple alternative was therefore developed as part of the Experiment Plan prior to analysing the rainfall, which defined this footprint in terms of 'corridors' placed symmetrically about each ATLANT™ site and oriented downwind along the axis defined by the steering wind direction. The statistical analysis was conducted using a dynamic 60° downwind arc footprint model and a 30km dynamic downwind corridor footprint model based on daily steering wind direction, as specified in the pre-analysis plan. In all cases these footprints extended out 75km from the ATLANT™ sites (Figure 1-2).

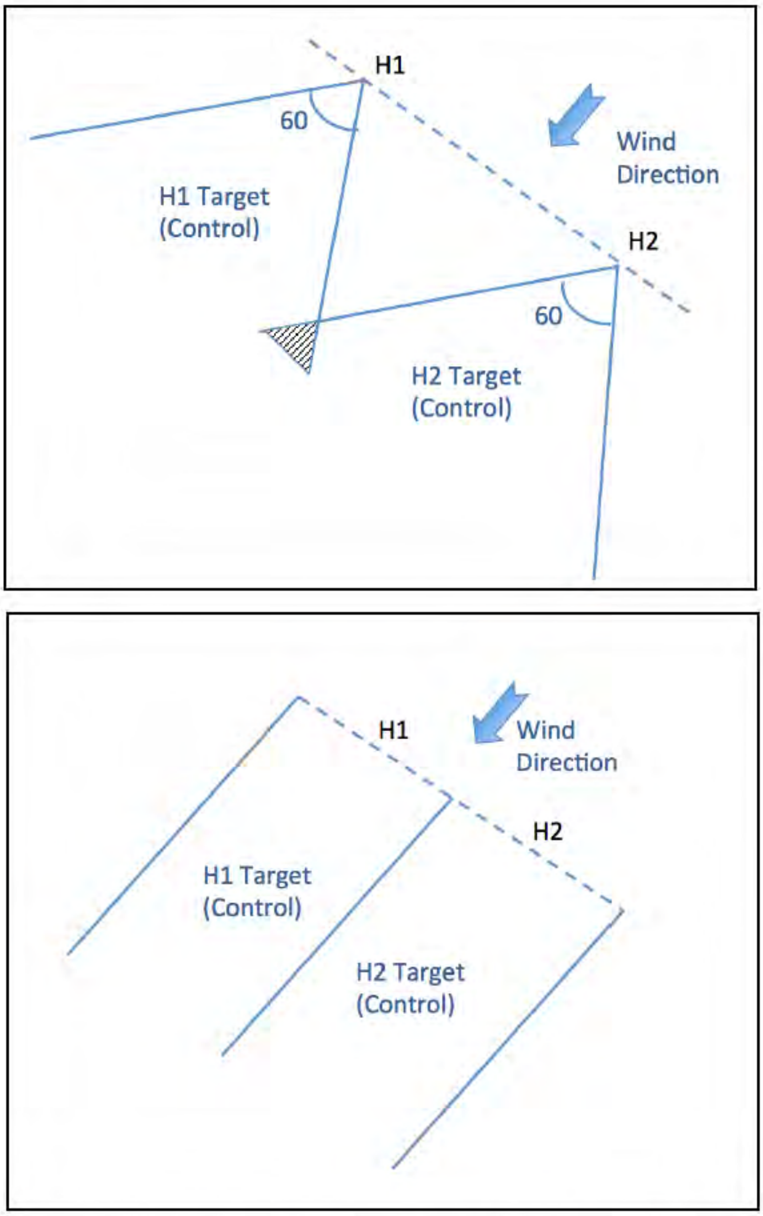

Figure 1-2 Dynamic 60° downwind wedge footprint model (top) and 30km dynamic downwind corridor footprint model (bottom)

1.2.3. Summary of results and recommendations of the 2013 trial

Overall, a positive and significant rainfall enhancement effect attributable to the operation of the ATLANT™ systems was observed over the course of the trial. The total attribution (enhancement effect) in the trial area defined by the wedge model, as a percentage of estimated natural rainfall, is estimated to be 11.7 per cent with a bootstrap standard error of 9.1 per cent. Furthermore, the bootstrap analysis indicates that this attribution is significantly greater than zero at a 90 per cent level of confidence, with a lower bound of 0.5 per cent for the bootstrap 90 per cent confidence interval for this attribution. Overall total attribution (enhancement effect) in the trial area defined by the corridor model, as a percentage of estimated natural rainfall, is estimated to be 18.0 per cent with a bootstrap standard error of 8.4 per cent. The bootstrap analysis indicates that this attribution is significantly greater than zero at a 99 per cent level of confidence, with a lower bound of 1.1 per cent for the bootstrap 90 per cent confidence interval for this attribution. The results are summarised below.

Table 1-1: Summary of 2013 trial results

Footprint Model	Mean level rainfall enhancement effect	Standard Error	Confidence level enhancement effect > 0
Corridor	18.0 %	8.4 %	99 %
Wedge	11.7 %	9.1 %	90 %

1.3. Substantive changes in the 2014 trial

Based on the positive results of the 2013 trial, further trials were recommended with the following suggested improvements in design:

1. Increasing the number of gauges in the prospective downwind target and control area that could in part be achieved by relocating upwind gauges;
2. relocating one or both of the ATLANT™s in order to provide a greater degree of separation of their footprints;
3. expanding the trial to include two or more additional ATLANT™s; and
4. installing upper air wind readings at H1 and H2.

Recommendations 1, 3 and 4 were implemented, with TIE relocating 12 gauges from the 2013 instrument array and installing 30 new gauges to complement the 2013 rain gauge array. Two additional ATLANT™s were commissioned in an expanded trial area. SODAR vertical wind profilers were installed at H1 and H2. Section 2 provides full description of the 2014 trial set up.

1.4. Structure of the report

This report first summarises the 2013 trial in Oman. Section 2 provides background meteorological background over the trial area, which shapes the trial design. The design of the 2014 trial is discussed in Section 3. Section 4 described meteorological conditions observed during the 2014 trial. Section 5 discusses how the ATLANT™ footprint (or area of effect) is defined in 2014. Section 6 provides description of the statistical modelling approach used in the 2014 trial. Similar to 2013 Oman trial, this approach controls for meteorological conditions and orographic effects with a view to reducing background noise. Section 7 describes the results of the modelling analysis, stating the estimated rainfall enhancement attributable to the operation of the ATLANT™. Section 8 concludes the report with a summary of its main findings and comments.

2. METEOROLOGICAL CHARACTERISTICS OF THE TRIAL AREA

2.1. Regional Climate

The Climate in the Sultanate of Oman varies from one region to another and from one season to another but can be divided mainly into two seasons, with transition months separating them, namely:

- Winter or Northeast Monsoon (December-March)
- Transition Northeast-Southwest Monsoon (April-May)
- Summer or Southwest Monsoon (June-September)
- Transition Southwest-Northeast Monsoon (October-November)

Past climatological studies have identified the winter season (December through March) as accounting for the bulk of rain in flat and coastal areas in northern Oman. Troughs, depressions, and the occasional tail end of cold fronts move through the region from the west and northwest resulting in large-scale systems that can provide significant rainfall. However the occurrence and amount of rainfall is highly variable, not occurring at all in some years, and provides few opportunities for regular rainfall enhancement operations.

2.2. Meteorological conditions over the trial period

During the summer season (June through September), convective rainfall over the Oman Mountains is a locally observed phenomenon that is known locally and has been recently studied. The reported high occurrence of convective storms over the Oman Mountains with consistently suitable microphysical conditions makes the summer season the most suitable time for rainfall enhancement operations.

2.2.1. Summer Orographic convection and precipitation

The Hajar Mountain range (Figure 2-1) is a key factor in inducing a significant amount of rainfall during summer months. These steep mountains have peaks of over 3000 metres, and run parallel to the coast of the Gulf of Oman. Convective clouds form over the mountains creating a regular occurrence of showers and thunderstorms over a limited area in northern Oman during the summer months (Figure 2-2 and Figure 2-3). The active weather is generally of short duration and intense. Orographic forcing, the advection of moisture from the south-western parts of the Arabian Sea or via sea breeze from the Gulf of Oman and large scale lifting are important factors in determining the occurrence of cloud and rainfall.

On days with no rain potential, dry north-westerlies converge (over the mountains) with the sea-breeze from the Gulf of Oman. Conversely on days with cloud and/or rain development, the sea-breeze converges with moisture flow advected from the Arabian Sea. A dry desert air will lead to moist convection being suppressed, whereas moist air advected from the Arabian Sea will enhance moist convection. Moisture advection from the Arabian Sea in a column of at least 1 kilometre in depth is required for proper convection (Al-Maskari et al. 2006). The stronger the flow from the Arabian Sea and the deeper the column of the moist air, the heavier the precipitation. Generally clouds that develop over the mountain peaks dissipate as they move west.

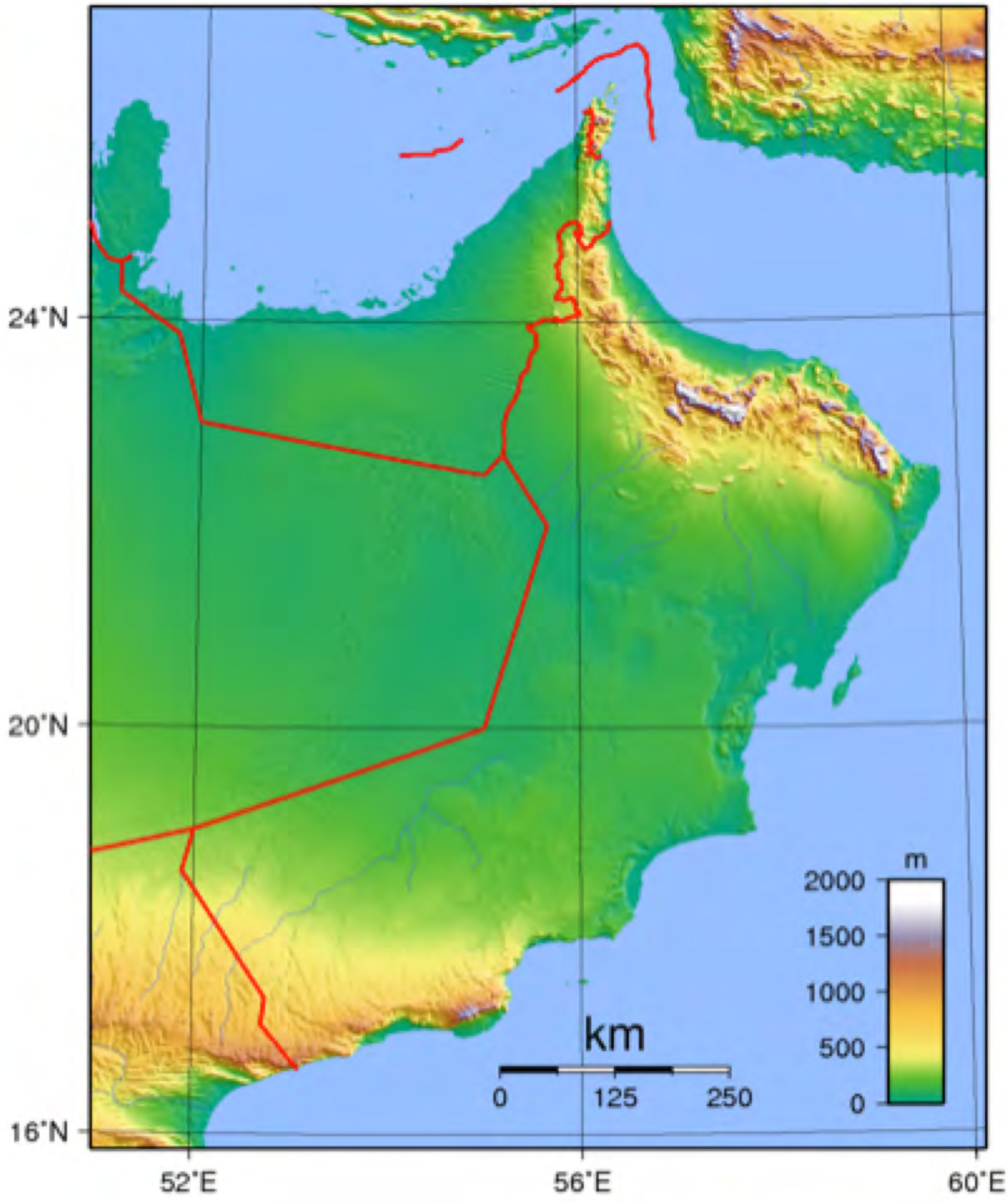

Figure 2-1 Hajar Mountains, Oman (at the top of the figure running WNW-ESE)

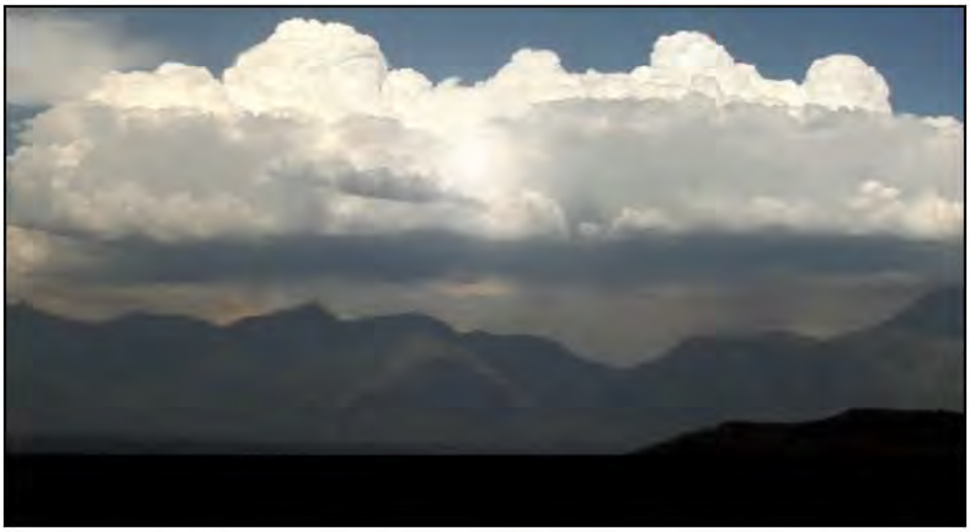

Figure 2-2 Convection clouds Hajar Mountains, Oman.

Figure 2-3 Convection along Hajar Mountains 10 July 2004 (source: Al Brashdl 2007).

3. 2014 TRIAL SET-UP

3.1. Trial Schedule

The operational schedule of the main trial activities is set out below:

- 01 March – 31 May 2014: Planning, transport, set up, testing of ATLANT™ systems
- 01 June – 18 October 2014: Operation of ATLANT™s, collection of field data
- 18 October – 31 January 2015: Analysis of data and preparation of final report
- February 2015: Presentation of final results to TIE.

3.2. Instrumentation of the trial

3.2.1. ATLANT™ Sites

Two new ATLANT™ sites (H3 and H4) were chosen to supplement the two ATLANT™ sites (H1 and H2) used in 2013 (Figures 3-2 to 3-5). The sites were chosen based upon the following criteria:

- The sites were as similar as possible, in terms of meteorological conditions, and elevation
- The ATLANT™ systems were separated sufficiently from each other, such that their areas of influence did not significantly overlap
- The sites are located such that a line joining them runs at 90° to the major wind direction and so are located to take advantage of orographic lifting of the ion plume
- Surface-based measurements exist in the expanded trial area (e.g. rain gauge sites)

Figure 3-1 The ATLANT™ sites in the 2014 trial (shown as yellow triangles)

1.1.1.1 ATLANT™ Site Hajar 1 (H1)

- Latitude: 23°19'21.74"N, Longitude: 57° 7'23.15"E, Elevation: 2670 m

Figure 3-2 The ATLANT™ at Hajar 1 Site

1.1.1.2 ATLANT™ Site Hajar 2 (H2)

- Latitude: 23°14'17.99"N, Longitude: 57°36'33.22"E, Elevation: 2157 m.

Figure 3-3 The ATLANT™ at Hajar 2 Site

1.1.1.3 ATLANT™ Site Hajar 3 (H3)

- Latitude: 23°41'32.65"N, Longitude: 56°48'6.42"E, Elevation: 1621 m.

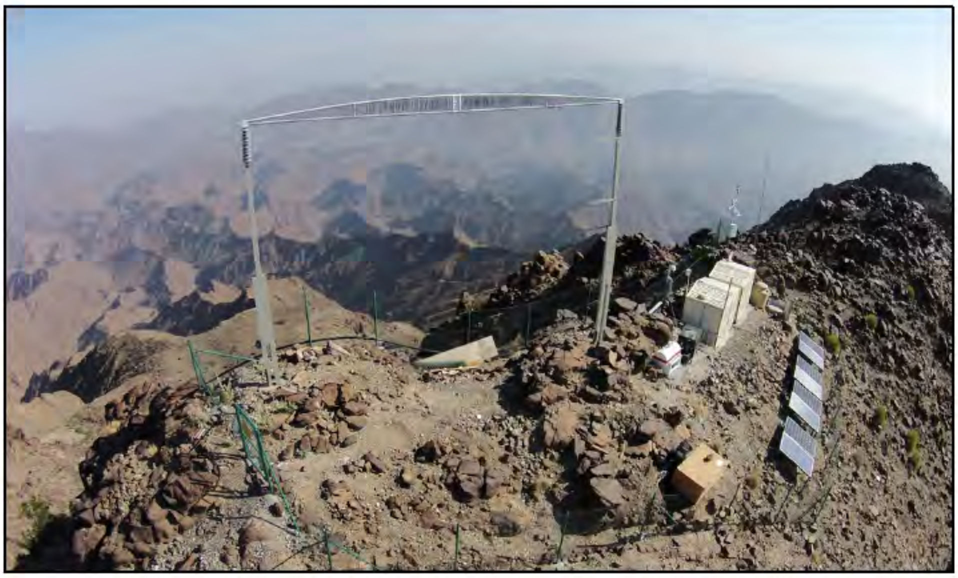

Figure 3-4 The ATLANT™ at Hajar 3 Site

1.1.1.4 ATLANT™ Site Hajar 4 (H4)

- Latitude: 23°10'23.73"N, Longitude: 58°2'40.8"E, Elevation: 1395 m.

Figure 3-5 The ATLANT™ at Hajar 4 Site

1.1.1.5 New ATLANT™ Design

H1 and H2 were of the same design as used in the 2013 trial, operated form the same locations. The two new ATLANT™s designated H3 and H4, were constructed using a new design. This design is shown in Figure 3-6 includes a simplified structure and uses ultra thin finer wire. Tests in Australia demonstrated that this design can produce up to 100% more ions than the original ATLANT™s. In addition this structure can be constructed within a small footprint as at remote sites H3 and H4.

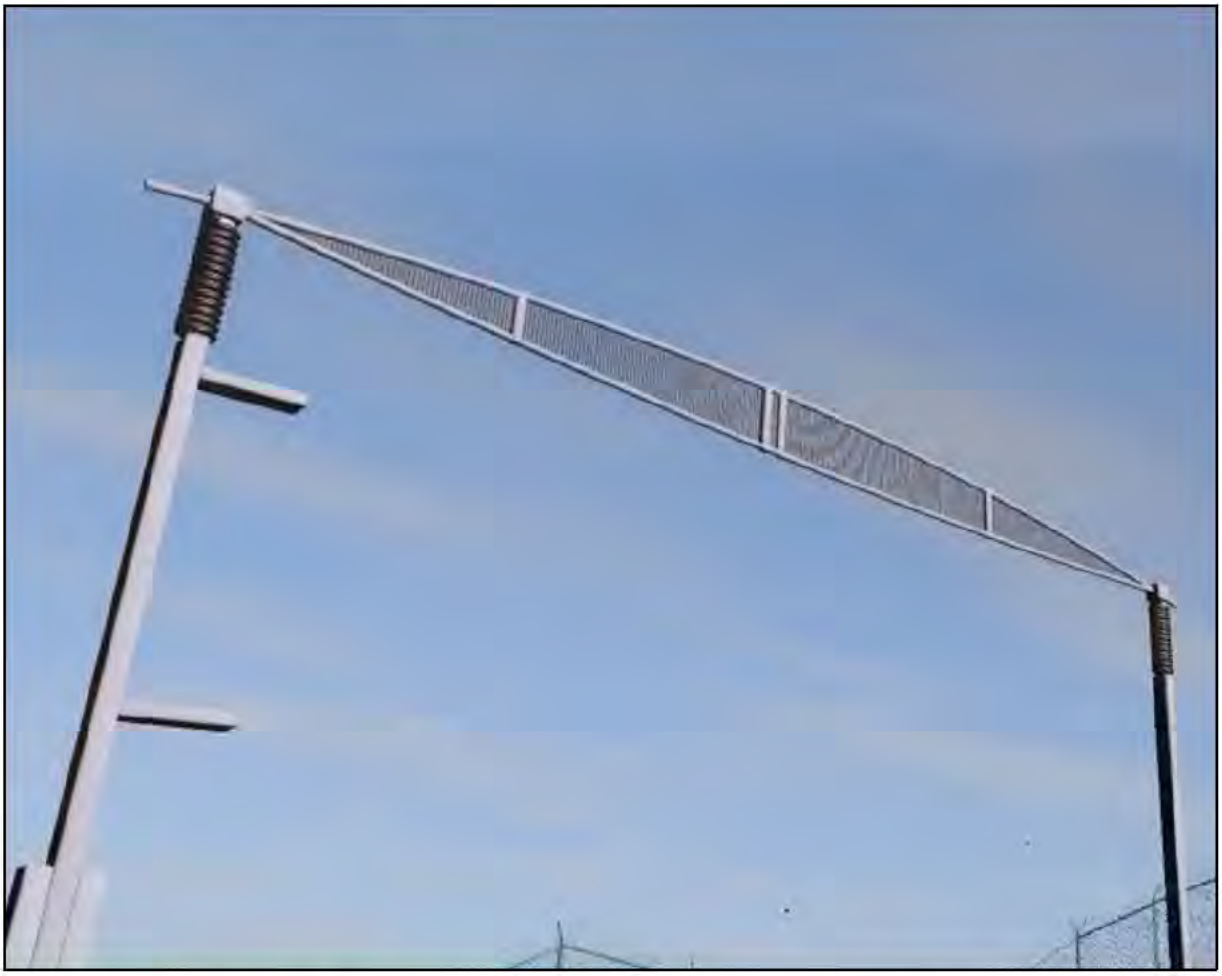

Figure 3-6 The New ATLANT™ at Hajar 3 and 4 Sites

3.2.2. TIE Rain gauge data

Rain gauges operated by the Oman Directorate General of Meteorology and Air Navigation (DGMAN) in the trial area are co-located with their weather observation sites, and hence limited in number. Due to the localised and short-lived nature of rainfall throughout the trial area, an extensive array of quality rain gauges was installed by TIE to supplement those operated by the DGMAN. In the 2013 trial, TIE installed an extensive array of rain gauges at approximately 10 km grid spacing. The 2013 final trial; report identified gauges (particularly upwind of the ATLANT™ sites) that did not contribute significantly to the analysis and would not be expected to contribute to analyses of future trials. These gauges were relocated for the 2014 trial. The addition of two ATLANT™ s H3 and H4 required additional gauges to be installed to cover their expected area of influence. TIE has used 12 relocated gauges from the 2013 array, as well as installing 30 new gauges to complete the 2014 rain gauge array. In total there were 149 gauges for the 2014 trial as depicted in Figure 3-7). These gauges provided rainfall data on an hourly basis.

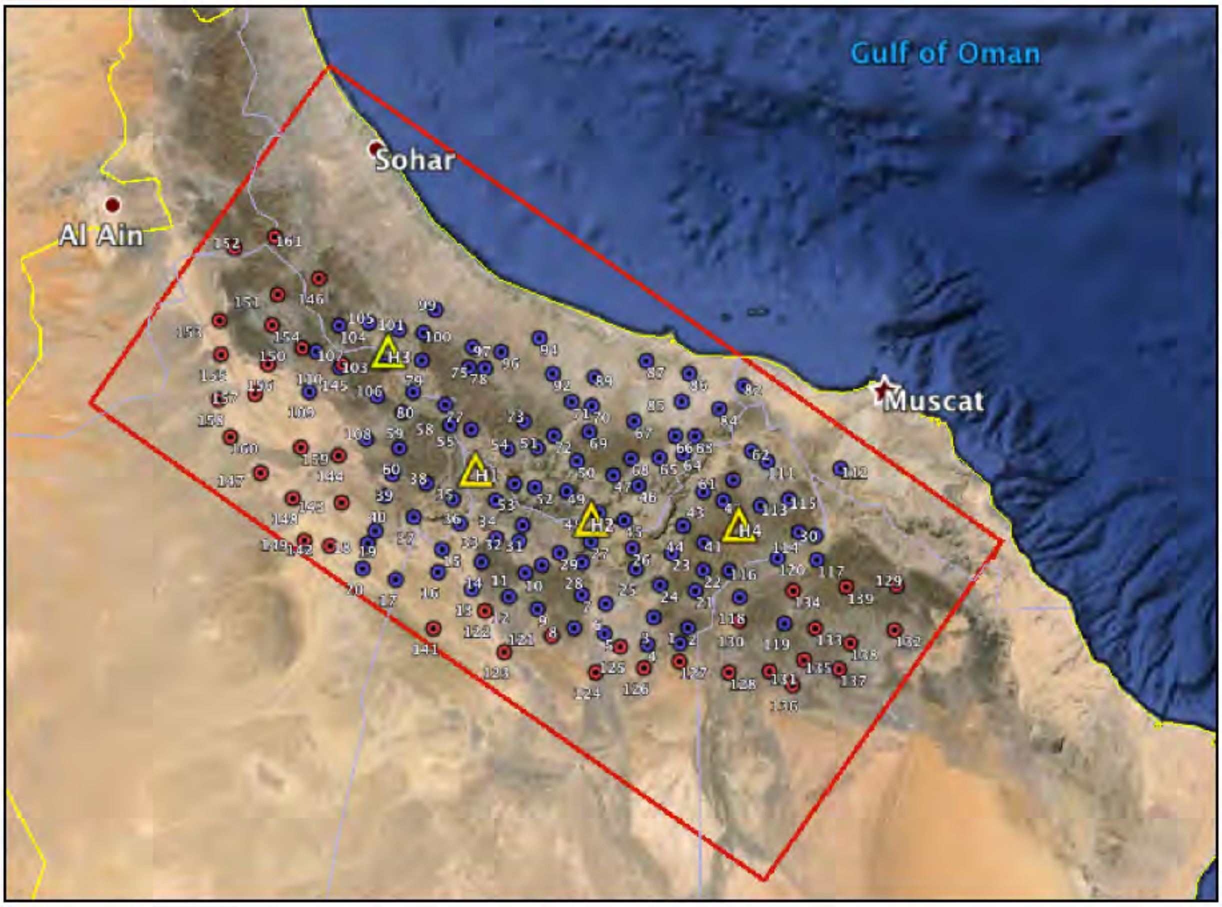

Figure 3-7 TIE Rainfall gauges installed in the Trial Area for 2014. ATLANTs are yellow triangles. 2013 Gauges in blue and new gauge locations in red.

3.2.3. TIE SODAR

Hourly upper air SODAR data was obtained from the H1 and H2 sites through TIE installed and operated Scintec MFAS SODAR systems (Figure 3-8) These acoustic profilers provide measurements of wind and turbulence up to 1000 m above the ground. The data output includes but is not limited to wind speed and direction, mixing height estimation and turbulence parameters. The operation of these systems is based on the reflection of acoustic pulses by temperature inhomogeneities in the air with subsequent doppler analysis.

Figure 3-8 TIE SODAR installed in the trial area

3.2.4. Seeb upper air sounding data

The Oman Directorate General of Meteorology and Air Navigation (DGMAN) operates a radiosonde at Seeb International Airport.

- Designator: 41256 Seeb Intl/Muscat
- Latitude: 23.35N
- Longitude: 58.17E
- Elevation: 8 m

This provides daily vertical soundings that were used to provide representations of the vertical wind profiles at the sites. Hajar 1 is located approximately 114 km to the west-southwest of the airport. Hajar 2 is located approximately 75 km southwest of the airport. The launch occurs at 00z daily (4am local time) and generates graphic and textual output at pressure levels during the balloon ascent. The station is equipped with Vaisala's Digicora GPS wind finding system and the radiosonde used is Visalla RS92 equipment.

1.1.1.6 Derived indices

In addition to the upper air wind speed and direction measurements obtained via the Seeb radiosonde, it was also possible to use the data from this source to derive daily moisture and stability indices. The following indices were therefore calculated and used in the statistical analysis:

- Total Totals Index (TT) (Miller 1972)
- Lifted Index (LI) (Galway 1956)
- Precipitable Water (PW)
- Convective Available Potential Energy (CAPE)
- LCL (Lifting Condensation Level)

3.2.5. Surface meteorological data

1.1.1.7 DGMAN AWS

There were 13 DGMAN weather stations with data over the trial period, with 10 stations providing almost complete data. These were Al Amrat, Al Mudhaibi, Bahla New, Ibri, Jabal Shams, Majis, Nizwa, Rustaq, Saiq, Saiq New, Samail, Samail New, Suwaiq. Hourly measurements of Dry Temperature, Dewpoint Temperature and Relative Humidity were available.

1.1.1.8 TIE AWS

In addition, TIE installed two Automatic Weather Stations at the new ATLANT™ sites (see Figure 3-9). These stations recorded the following data:

- Rainfall total
- Air temperature
- Air humidity
- Wind direction
- Wind speed
- Air pressure
- Radiation
- Evaporation

Figure 3-9 TIE Automatic Weather Station at H2

3.3. Final Instrument Array

All the meteorological instruments described above collected data during the operating period. The full instrument array is depicted in Figure 3-10, including their elevation and location.

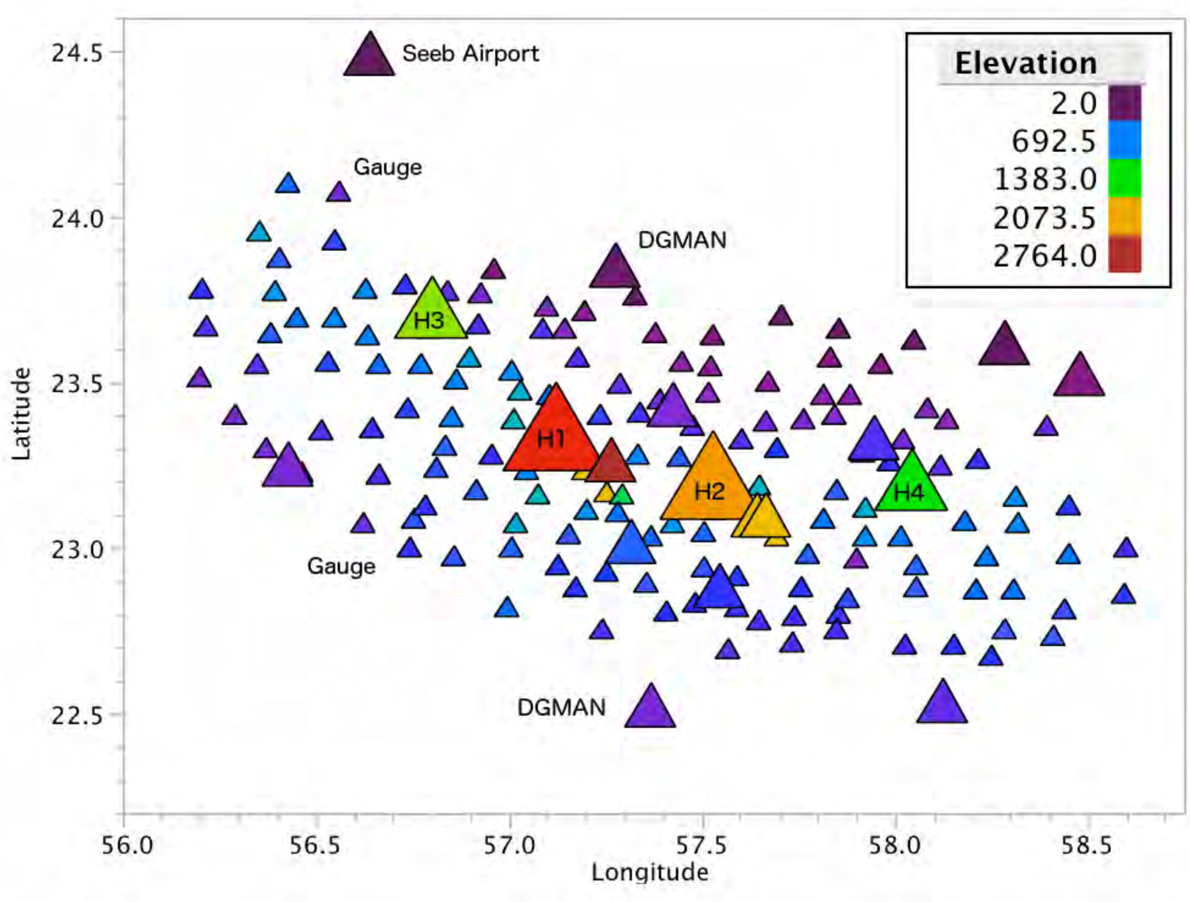

Figure 3-10 Instrument array. (Rain gauges – small triangles. Surface weather stations- medium triangles. ATLANT™s / TIE Weather stations large triangles. Elevation is colour scale in metres.

The data recorded and available for use in the analysis is detailed in Table 3-1.

Table 3-1 Final data

Instrument	Parameter	Frequency	Notes
TIE Rain Gauge	Rain total	Hourly	148 Gauges no missing data 1 gauge with missing data
H1 Weather Station	Wind speed	Hourly	15 May – 31 October
	Wind direction	Hourly	15 May – 31 October
	Temperature	Hourly	15 May – 31 October
	Humidity	Hourly	15 May – 31 October
	Evaporation	Hourly	15 May – 31 October
	Radiation	Hourly	15 May – 31 October
H2 Weather Station	Wind speed	Hourly	17 May – 31 October
	Wind direction	Hourly	17 May – 31 October
	Temperature	Hourly	17 May – 31 October
	Humidity	Hourly	17 May – 31 October
	Evaporation	Hourly	17 May – 31 October
	Radiation	Hourly	17 May – 31 October
Seeb Radiosonde	Wind speed Wind direction Total totals LCL CAPE Lifted Index Precipitable-Water	Daily	4am (500 Hpa/700 Hpa) 15 May – 31 October 24 days missing
DGMAN Stations Al Amrat, Al Mudhaibi Bahla New, Ibri Jabal Shams Majis, Nizwa Rustaq, Saiq Saiq New, Samail Samail New, Suwaiq	Rain total Wind speed Wind direction Temperature Humidity Evaporation Radiation	Hourly	15 May – 31 October Some missing data but over 90% complete

3.4. Experiment Design

The 2014 trial employed a randomised crossover design (similar to the 2013 trial). The crossover design applied to the trial had two pairings of ATLANT™ sites operate on a randomly predetermined rotation basis throughout the trial with no breaks. That is Hajar 1 (H1) and Hajar 4 (H4) formed one group and operated together, and Hajar 2 (H2) and Hajar 3 (H3) formed the second group and operated together. This had two main benefits:

- All ATLANT™s were already established and operated from 01 June. Grouping an 'old' ATLANT™ with a 'new' ATLANT™, meant the operating scheduled could be seamlessly maintained when the 'new' ATLANT™s commenced operation.
- As noted in the 2013 final trial report, greater separation between ATLANT™s is desirable to minimise 'crossover' effects. In 2014, pairing the ATLANT™s meant the operating ATLANT™s were effectively 100 km apart.

3.4.1. Randomised operating schedule

The two groups of sites were operated in a randomised alternating schedule. Rather than randomly generating the schedules for H1/H4 and H2/H3 and then combining them, a schedule was constructed as follows.

The operating schedule for the 2014 Oman ATLANT™ trial first spatially blocked over two days A and B, as indicated in Table 3-2.

The operating schedule was then blocked temporally into balanced 14-day blocks. The daily schedule with 10 blocks is shown in Table 3-3 with 1 designating an 'A' day and 0 designating a 'B' day.

Table 3-2: Spatial layout for the 2014 Oman ATLANT™ trial

Day	H3	H1	H2	H4
A	On	Off	On	Off
B	Off	On	Off	On

Table 2-3: The balanced 14 operating schedule for 10 blocks, B1 to B10

Day	B1	B2	B3	B4	B5	B6	B7	B8	B9	B10
1	0	1	0	0	1	0	0	0	1	0
2	1	1	0	1	0	1	1	0	0	1
3	0	0	0	0	1	1	1	1	0	0
4	1	1	1	1	0	0	1	0	0	1
5	0	1	1	0	0	0	1	1	1	1
6	0	0	0	1	0	1	0	0	1	0
7	1	1	1	1	1	0	0	1	1	0
8	1	0	0	1	0	1	1	0	0	1
9	1	0	0	1	0	1	0	1	1	0
10	0	0	0	0	1	0	0	0	1	1
11	0	0	1	1	0	0	0	1	1	0
12	0	1	1	0	1	1	1	1	0	0
13	1	0	1	0	1	0	0	0	0	1
14	1	1	1	0	1	1	1	1	0	1

The operating schedule was then constructed from the 10 blocks B1-B10 consecutively commencing from 01 June. An advantage of this approach was to ensure that each combination is scheduled for an equal number of days yielding 70 'A' days and 70 'B' days. The operating schedule commenced 01June 14 and was completed 18 October 2014.

The full planned operating sequence is detailed at Annex A.

3.4.2. Faults and non-operational days

In the 2014 trial there were instances when an ATLANT™ system was scheduled to operate but did not operate due to technical faults or in accordance with the experiment risk management plan. If both the operating ATLANT™ systems failed to operate within the window from 10:00 to 18:00, the day would be excluded and the schedule would not advance (the excluded day would be repeated). If at least one of the planned operating ATLANT™ systems operated for some period (1 hour) within the window from 10:00 to 18:00, the schedule advanced as planned.

3.4.3. Defining Switch Time

As for 2013 trial, the nominal switch time is (07:00) 7am local time. The operating ATLANT™ were turned off at (06:30) 6.30am to let the ions clear away. The ongoing ATLANT™ was turned on at (07:00) 7am daily in accordance with the planned operating schedule.

3.4.4. Target/Control area definition

The determination of the Target/Control area took the same approach as used in the 2013 trial (see 2013 Experiment plan for further detail). However in 2014, two SODAR (SOnic Detection And Ranging) wind profilers were installed and operated by TIE at H1 and H2. Measurements from these systems were used in conjunction with upper air sounding profiles at Seeb airport obtained from Oman Directorate General of Meteorology and Air Navigation (DGMAN), and used to estimate steering wind direction and in turn define target and control areas. For complete definition of the target/control determination for the 2014 trial, see Section 5.

4. METEOROLOGICAL CONDITIONS OBSERVED DURING THE TRIAL

Metrological conditions that prevailed over the trial area are presented in this section of the report. These conditions include:

- Precipitation
- Wind direction and speed
- Other potential covariates for use in the statistical modelling to control for the natural spatial and temporal variation in rainfall

4.1. Precipitation

Daily rainfall statistics for the trial are shown in Table 4-1. The data is from the 149 gauges installed by TIE in the trial area. There was at least some rainfall recorded on the majority of days in each month of the trial. In general, rainfall was not widespread on any given day for the entire trial, with the average daily percentage of gauges recording rainfall over the trial period equal to 8.7 per cent.

June through September of the trial period followed the expected pattern with more widespread and higher average gauge level rainfall in July and August, preceded and followed by lower recordings in June and September. The high frequency and levels of rainfall recorded in October appear to be uncharacteristic.

A plot of the cumulative number of gauges against the number of days that rainfall was recorded at a gauge is shown in Figures 4-1. Roughly one third of the gauges recorded eight rainfall days or less, one third recorded over 8 but less than 15 rainfall days and the last third 15 days or more. No gauges recorded rainfall on more than 35 days of the 141-day trial. It appears that convective cloud formation and precipitation in the trial area is spatially localised and variable.

A histogram of total rainfall recorded at each gauge is shown in Figure 4-2. The distribution of total gauge rainfall exhibits a pattern similar to what is commonly observed for rainfall at a single site over time. There are a large number of gauges that recorded only small amounts of rain and a long tail that extends through to a small number of gauges that recorded extremely high levels of rainfall.

Table 4-1. Summary daily rainfall statistics from the TIE gauge network for days when at least one gauge in the trial area recorded a rain event (Rainfall Days): 1 June to 18 October 2014

Period	Rainfall Days	Gauges Recording (%)	Mean Gauge Rainfall (mm)	Total Rainfall (mm)
June	19	4.5	3.50	748
July	22	7.6	4.82	1,697
August	30	13.0	5.23	3,144
September	27	6.9	2.65	820
October	16	12.1	4.13	1,424
Total	114	8.7	4.30	7,832

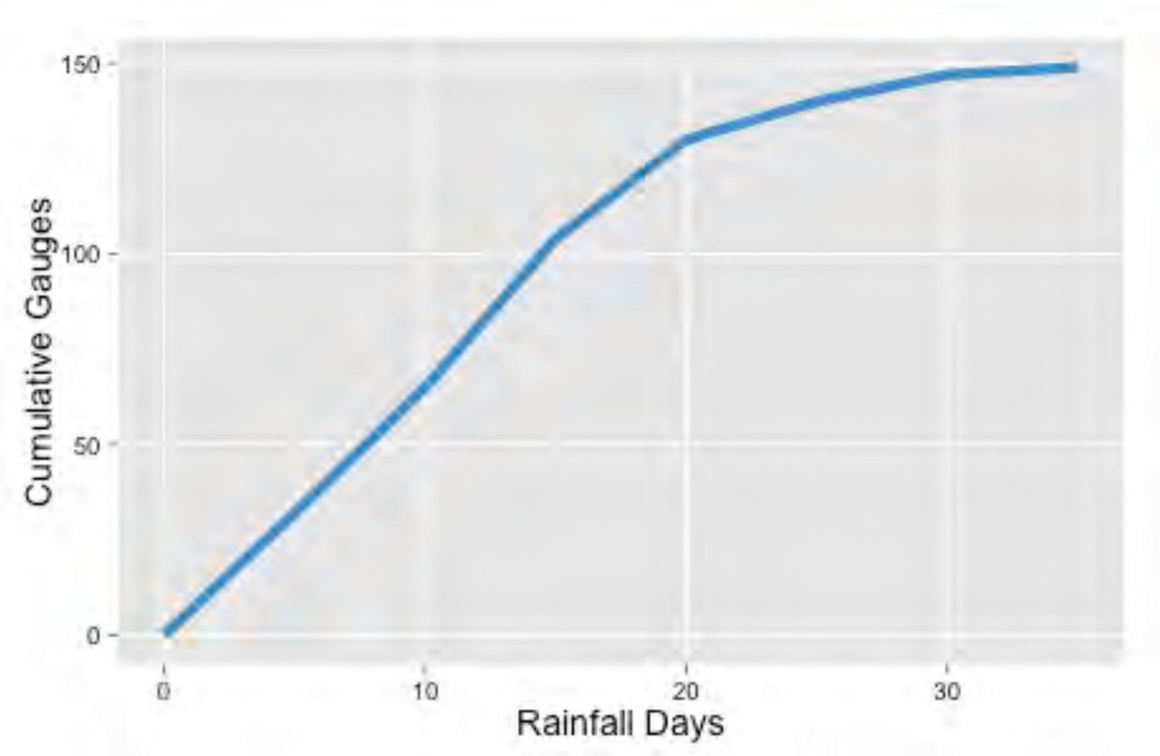

Figure 4-1. Gauge counts and number of days that rainfall was recorded at the TIE gauges: June to 18 October 2014.

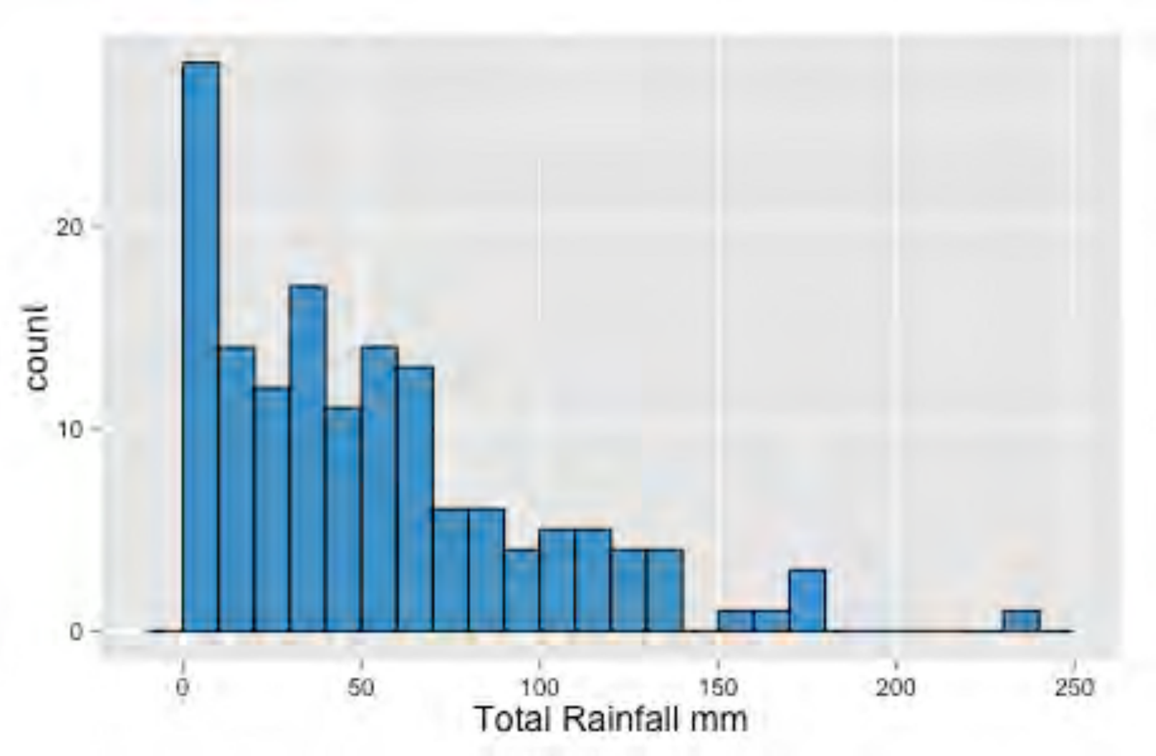

Figure 4-2. Total rainfall recorded at the TIE gauges: 1June to 18 October 2014.

The next graph (Figure 4-3) in this section of this report is a bubble plot in which the bubbles are located at the locations (latitude and longitude) of the gauges, the bubble size indicates how frequently a gauge recorded rain and the colour of the bubble indicates the total rainfall for the gauge. Rainfall is less frequent along the coast and increases moving up along the windward side of the Hajar Mountains. From the crest of the ranges down the leeward side of the ranges rainfall frequency remains relatively high. Moving from northwest to southeast, the principal axis of the ranges, rainfall frequency is again consistent. However, substantially more rainfall fell in the northwest.

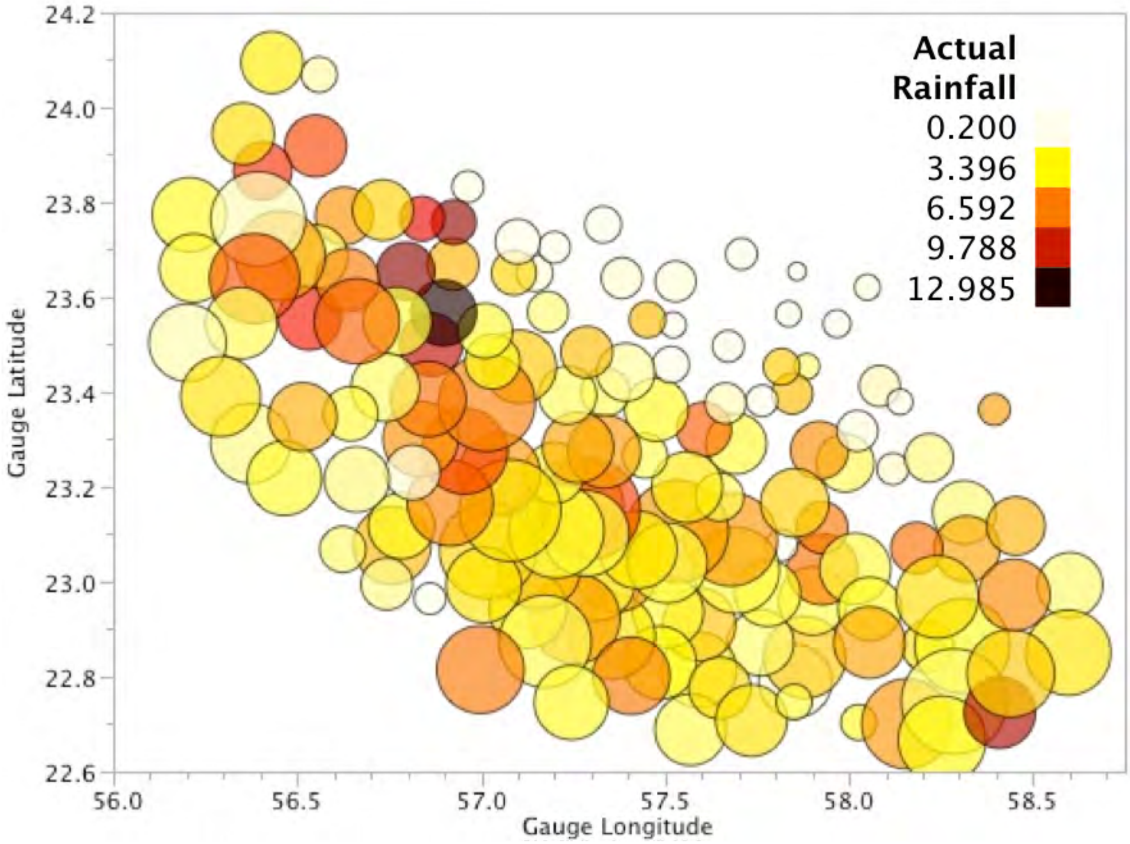

Figure 4-3. Bubble plot of the locations of the TIE rain gauges, with gauge rainfall frequency proportional to bubble size and gauge total rainfall (Actual Rainfall) denoted by the colour scale shown: 1 June to 18 October 2014.

4.1.1. Spatial and Temporal Correlation

The choice between conducting rainfall analysis on the basis of regional averages or at the gauge level depends in large part on the correlation between rainfall observations at the different gauge sites. The greater the degree of spatial and temporal independence of rainfall observations, the greater is the efficiency gain in using gauge level data. Given the low level of correlation between gauge observation, the larger sample size of gauge as opposed to regional averages is less likely to understated the errors associated with statistical estimates.

This correlation may be spatial and temporal. If rainfall tracks in the direction of prevailing winds that vary from day to day this may also introduce spatiotemporal correlation. However, our concern is limited to spatial and temporal correlation.

The level of spatial correlation in non-zero daily rainfall observations is shown as a function of gauge distance in Figure 4-4. It is clear that even over relatively short distances correlations are relatively low and decline quickly as distance increases. The distribution of first order temporal correlation at each of the gauges is shown in Figure 4-5. These values are based on data that includes zero and positive rainfall observations. Overall the trade-off appears to strongly favour gauge level analysis. It should be noted that the interaction between space and time, as for example though the current wind direction and distance, can also introduce correlations. Consequently spatiotemporal variability (i.e. day to day change in spatial variability) still needs to be taken into account.

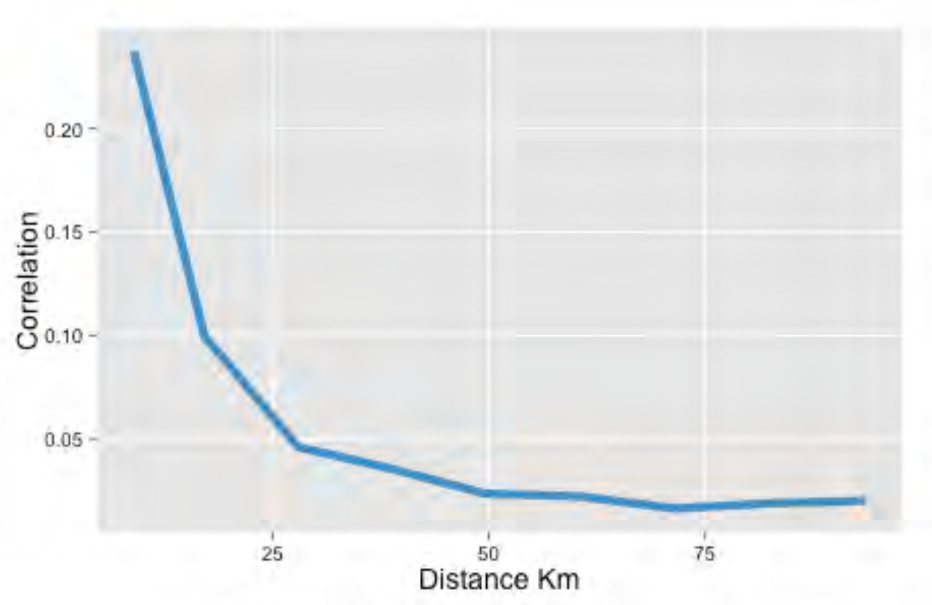

Figure 4-4. The correlation between positive rainfall observations as a function of the distance between rainfall gauges.

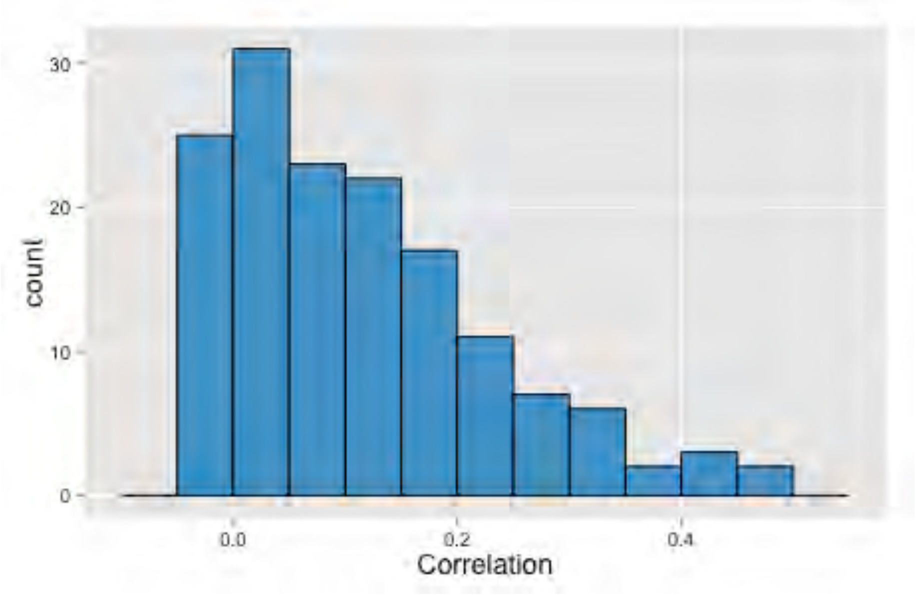

Figure 4-5. The first order temporal correlation between rainfall observations at the TIE rainfall gauges.

4.2. Upper Level Winds

Prevailing wind conditions in the trial are summarised in the following two graphs which are based on radiosonde data from Seeb airport and daily average wind speed and direction data from SODARs installed at H1 and H2. Wind readings at Seeb are across two pressure ranges, a high level reading at 500hPa to 700hPa and a middle level reading form 700hPa to 850hPa. Radiosondes are released once daily from Seep airport at 3am. The SODAR data are daily averages through a 50 to 400 metre vertical profile above H1 and H2. The SODAR at H2 was operational for the complete trial, while that at H1 became operational on August 5.

The distribution of daily speed weighted average wind directions is shown in Figure 4-6. In this figure, the proportion of observations from each site is shown for the eight points of a compass rose. There are clear prevailing wind directions at each site. High-level winds at Seeb generally range from north to east, coming out of the northeast over 40 per cent of the time. There is a westward shift in the lower level wind direction at Seeb and at H2. There is an easterly shift at H1. These shift give an indication of the complexity of the orographic influences of the Hajar Mountains, along and well in front of the ranges.

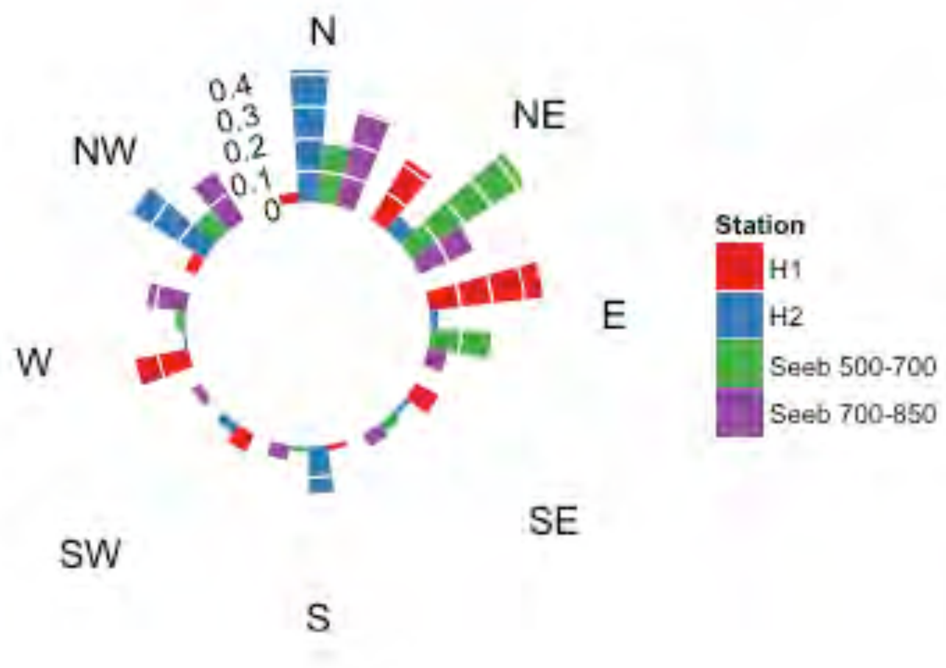

Figure 4-6. The distribution of daily upper level wind directions at Seeb airport, H1 and H2: speed weighted averages.

Average wind speeds are shown in Figure 4-7. The difference in speeds between the upper elevations at Seeb and surface influenced winds at lower elevations is clear at each point of the compass rose. However, the average wind speed at each site does not differ substantially with direction.

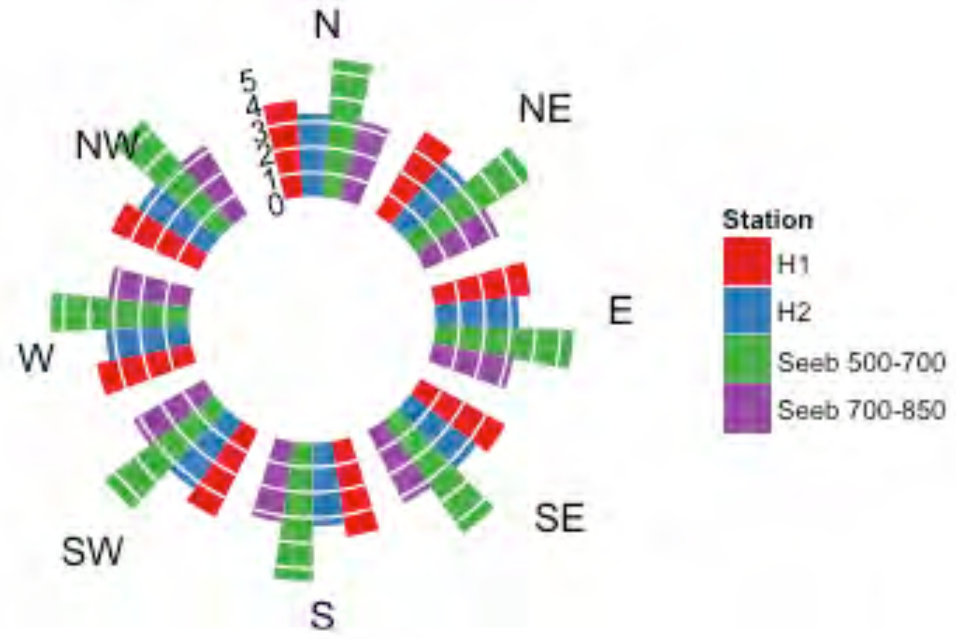

Figure 4-7. Daily average wind speeds in metres per second at Seeb airport, H1 and H2.

4.2.1. Correlations

While is it clear that there are differences in the prevailing wind directions at each site due to the orographic influences of the Hajar Mountains, orographic effects will also affect the correlation between wind flows. To calculate this correlation structure, daily wind directions and speeds were converted to zone (east-west) and meridian (north-south) values. The correlation between these values is shown in figure 4-8, where u denotes the zone value and v the meridian value.

There is a moderate level of correlation between the zone values at each site and moderately strong correlations between the meridian values. There are only a few substantial cross correlations between the two sets of values. The zone value at H1 is strongly correlated with the meridian value at H2 and the correlation between H1 and the lower level Seeb meridian values is moderately strong. There is a moderately strong inverse correlation between the zone value at H2 and the meridian value at H1.

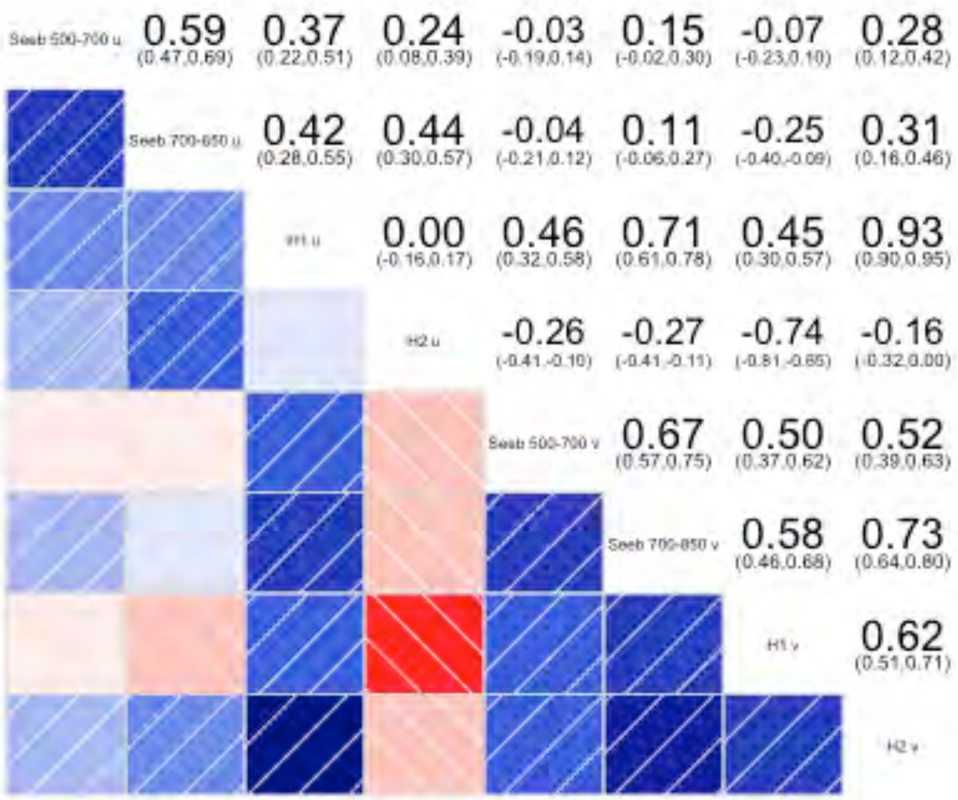

Table 4-8. The correlation structure of wind zone (u) and meridian (v) values at Seeb, H1 and H2

4.3. Potential Meteorological Covariates

The distributions of two sets of potential metrological covariates are explored visually in this section. The first set is surface measurements from the automated DGMAN weather stations operated by the Oman Bureau of Meteorology. The second set is from the SODARs installed at H1 and at H2. Note that information is provided for all 13 DGMAN stations, whereas the statistical modelling of rainfall in the 2014 trial that is described later uses only data from the 10 stations (see Table 3-1) with complete records over the trial period.

4.3.1. DGMAN Meteorological Data

There are 13 DGMAN stations in the trial area that record hourly observations on dewpoint, relative humidity, temperature, surface wind direction and speed. These hourly measurements were restricted to between 10am and 8pm and then averaged. Dew point temperatures and relative humidity are shown in Figures 4-9 and 4-10.

There is a reasonable degree of variability in dew point temperature and relative humidity over time across the sites. Hence, these variables are potential covariates that may help control for the natural spatial variably in rainfall over the trial area. However, this will depend on the degree of spatial independence of the observations. If the observations at different sites are strongly correlated they will not be effective location specific controls for accounting for natural rainfall.

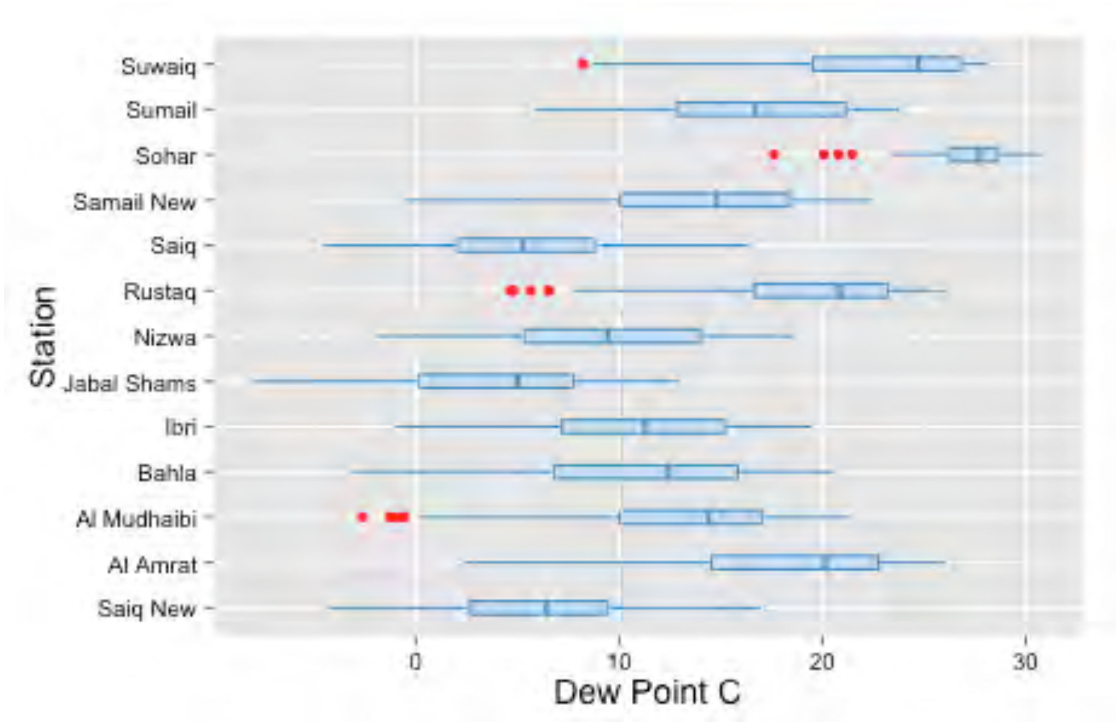

Figure 4-9. The distributions of daily (10am - 8pm) dew point temperatures at the 13 DGMAN weather stations: 1 June to 18 October 1014.

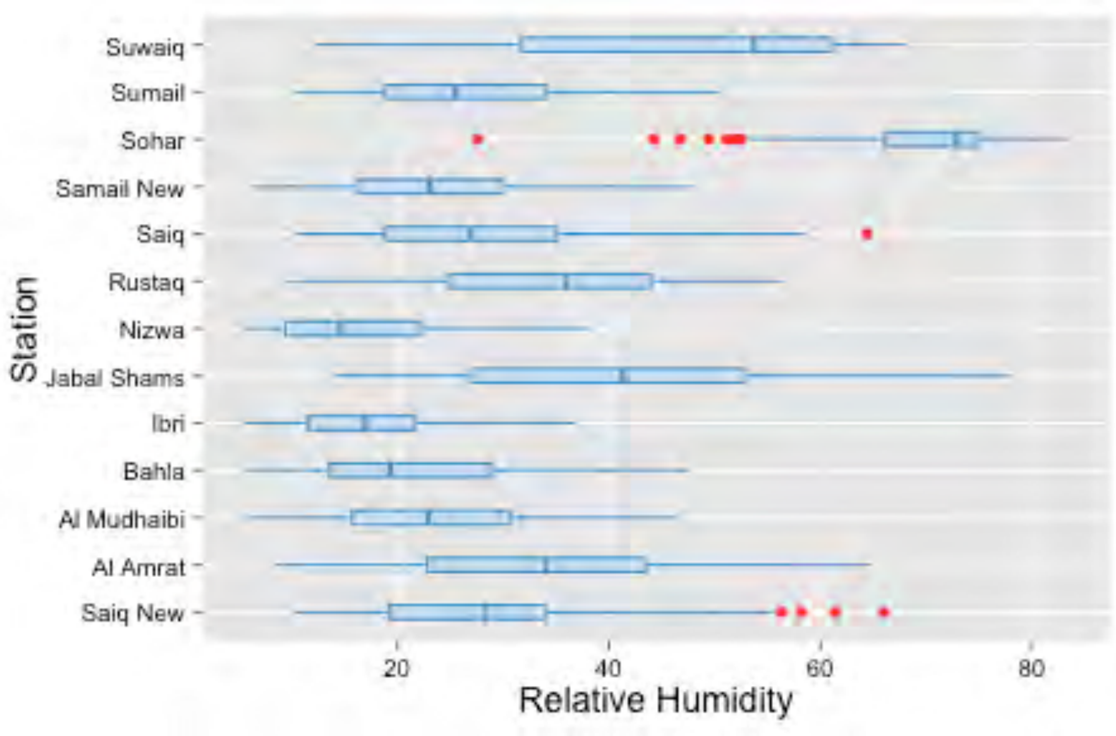

Figure 4-10. The distributions of daily (10am - 8pm) relative humidity at the 13 DGMAN weather stations: 1 June to 18 October 1014.

The distributions of the daily average zone and meridian wind values at each station are shown in Figures 4-11 and 4-12. There are considerable differences in the medians of these values as well as the extent of their variability at each site. This is in contrast to the more steady upper level wind readings at Seeb and the SODAR readings above H1 and H2. The zone values are split between easterly and westerly flows and the meridian wind values are split between northerly and southerly flows. Note that the variation is greatest in the east-west direction (the scales of the two figures differ).

Clearly surface winds are completely dominated by orographic effects and these orographic effects differ radically at different locations in the Hajar Mountains. This suggests that the observed differences in wind direction above H1 and H2 are to be expected throughout the ranges, implying nothing can be inferred from these data about the behaviour of the winds above H3 and H4 or any future site.

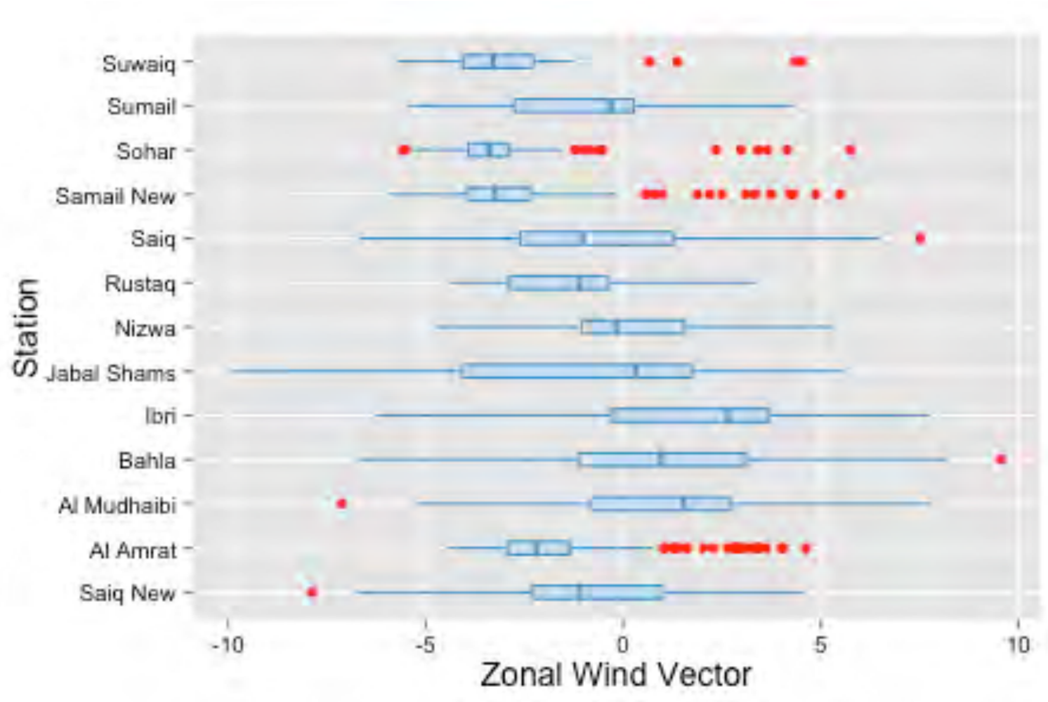

Figure 4-11. Daily zone values for the 10am - 8pm surface winds at the DGMAN weather stations: 1 June to 18 October

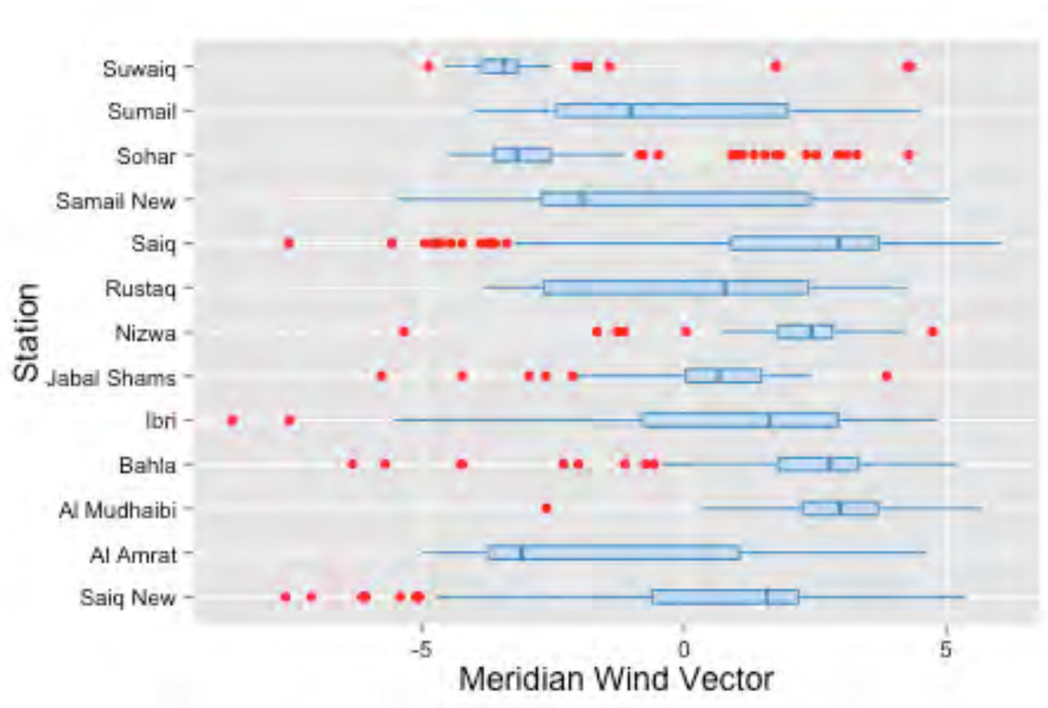

Figure 4-12. Daily meridian values for the 10am - 8pm surface winds at the DGMAN weather stations: 1 June to 18 October

4.3.2. SODARS

The SODAR wind profiles at H1 and H2 include:

- Horizontal wind speed
- Horizontal wind direction
- Vertical wind speed
- Temperature.

The distribution of average wind directions and speeds in the trial area has been explored previously. Information from the vertical profiles, while quite different at H1 and H2, may still provide proxy measures of the degree of orographic uplift over the mountain ranges in the trial area. That is, it could help differentiate between days with relatively higher or lower levels of orographic uplift. Daily averages and standard deviations were therefore calculated across the vertical profile between 10am and 8pm.

The average daily zone and meridian values from the vertical SODAR wind profiles are shown in Figure 4-13. The inversion of the vectors at H1 and H2 is quite apparent, with east to west zone values dominant at H1 and north to south meridian values dominant at H2. In contrast, the daily standard deviations of the wind vectors, i.e. the within day variation, are all quite similar, as can be seen in Figure 4-14.

The mean and standard deviation of vertical wind speeds from the vertical SODAR profiles are shown in Figure 4-15. Vertical wind speeds are higher at H1. While the day-to-day variability in wind speeds in similar at H1 and H2, the within-day variation is greatest at H1.

The mean and standard deviation temperature from the vertical SODAR profiles are shown in Figure 4-16. Temperatures are lower at H1, reflecting the higher elevation of the site. Within day variability in temperatures is small but still considerable greater at H1 compared with H2.

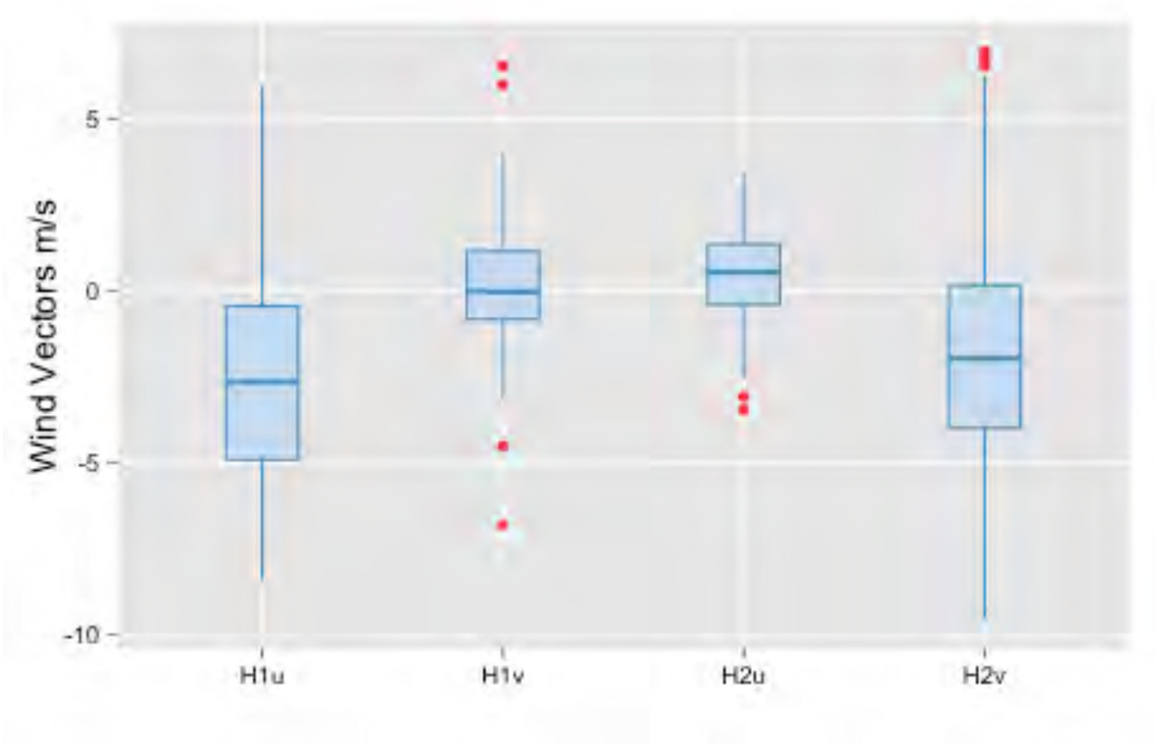

Figure 4-13. The distribution of the average daily zone (u) and meridian (v) wind values from the vertical SODAR profiles at H1 and H2

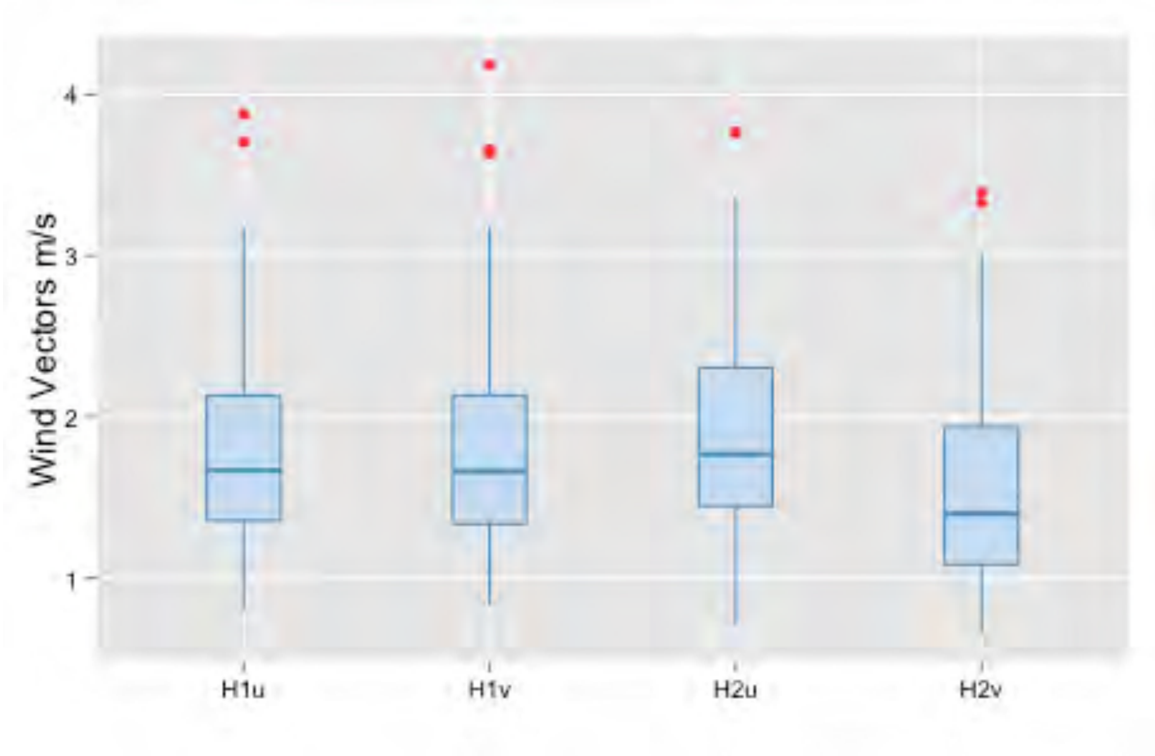

Figure 4-14. The distributions of the daily zone (u) and meridian (v) wind values from the vertical SODAR profiles at H1 and H2

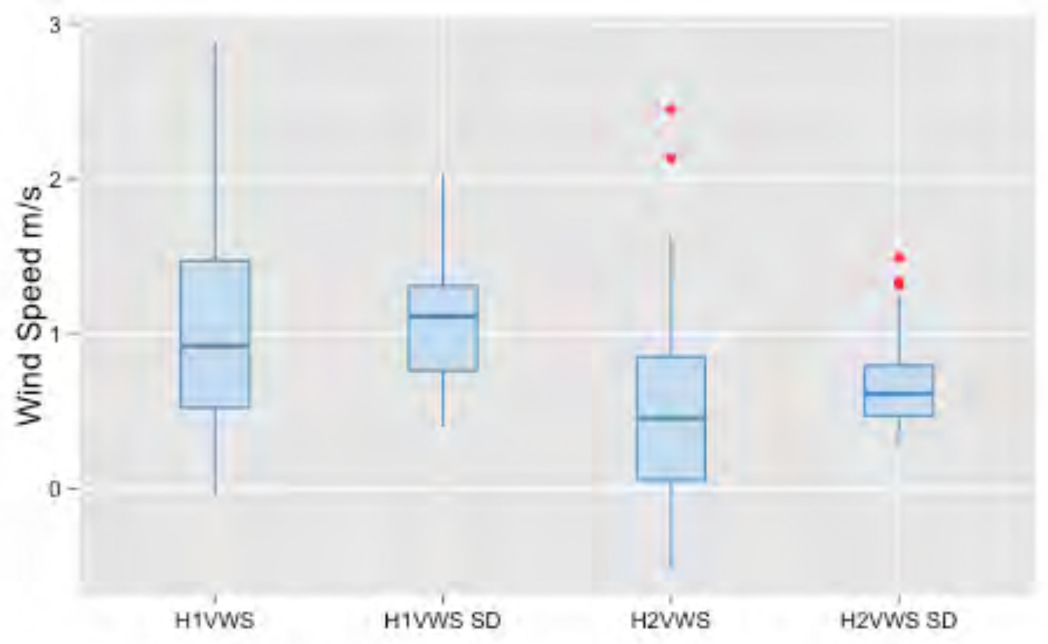

Figure 4-15. The distributions of the daily vertical wind speeds (VWS) and their within day standard deviations (VWS SD) from the vertical SODAR profiles at H1 and H2

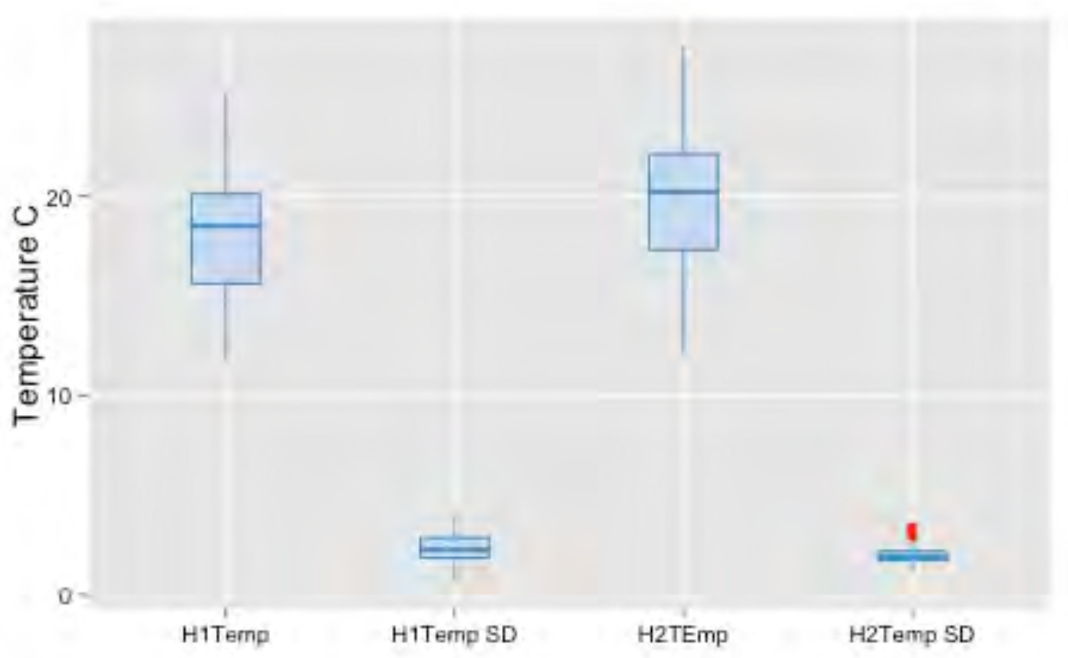

Figure 4-16. The distributions of the daily average temperatures (Temp) and their within day standard deviations (Temp SD) from the vertical SODAR profiles at H1 and H2

5. DEFINING THE ATLANT^{TM} FOOTPRINT

Daily classification of rainfall gauges, relative to the ATLANT^{TM} sites, as downwind targets and controls as well as those which are upwind of the sites, is a critical aspect of the statistical analysis. Whether or not a gauge is in an ATLANT^{TM} footprint on a particular day (i.e. could have recorded precipitation from clouds that had been exposed to an ion plume generated from an ATLANT^{TM} site on that day) is an unobserved or latent experimental condition. This footprint is assumed to be a function of wind direction and speed at the time convective clouds are formed due to the uplift of moist air by the Hajar Mountains on the day.

A particle plume generated by an ATLANT^{TM} emitter would initially be under the influence of lower level wind directions as well as horizontal and vertical speeds at a site. These are dominated by orographic features of the mountain terrain surrounding the site. These local influences would persist until the plume reached the upper limit of the atmospheric boundary layer, at which point the direction and speed of winds in the free atmosphere take over. Free air flows are generally stable, running roughly parallel to the pressure isobars one sees in a synoptic weather chart.

In the 2013 trial data from upper level winds above Seeb airport were used to determine the footprint. The SODAR and RSS data collected at the H1 and H2 sites during the 2014 trial has given a clearer picture of how complex these orographic effects are. These data also allow the height of the atmospheric boundary layer to be estimated and to create an approximate track of an ion plume. This provided an opportunity make a more critical assessment of how the footprint should be specified.

5.1. Height of the Atmospheric Boundary Layer

The height of the atmospheric boundary layer can be estimated approximately by the upper limit of RSS temperature profiles. The RSS emits radio waves and measures the signal returned to earth as it reflected back by the high concentrations of aerosols in the boundary layer. Radio waves passing through the boundary layer are not reflected back to earth, hence the boundary layer height is roughly where the signal is all, or for the most part, lost. The percentages of missing temperature observation at H1 and H2 are shown in Figures 5-1. The vertical axis of the graph can be interpreted as percentiles.

During the afternoon (i.e. 12pm to 6pm) the signal is completely lost at 650 metres above H1 and 870 metres above H2. This will be an over-estimate of the average height of the boundary layer, as most times the signal will be lost at lower elevations. In the afternoon, the average height at which the signal is lost is 340 metres at H1 and 510 metres at H2. The hourly distribution of boundary heights estimated by the loss of the RSS signal is shown in Table 5-1. The spread of the distribution is larger at H2.

Table 5-1 Percentiles of estimated height of the boundary lawyer above H1 and H2: 12pm to 6pm

Site	10th	20th	50th	80th	90th
H1	230	260	330	400	450
H2	330	400	520	610	650

Average vertical wind speeds by height are shown for H1 and H2 in Figure 5-2. Carried at these speeds it would take an ion plume about 4.5 minutes to reach an average boundary layer height of 340 metres at H1. To reach an average boundary layer height of 510 metres at H2 would take 20 minutes. At the 90th percentiles the time needed to reach the boundary height would be 7.3 minutes at H1 and 26 minutes at H2.

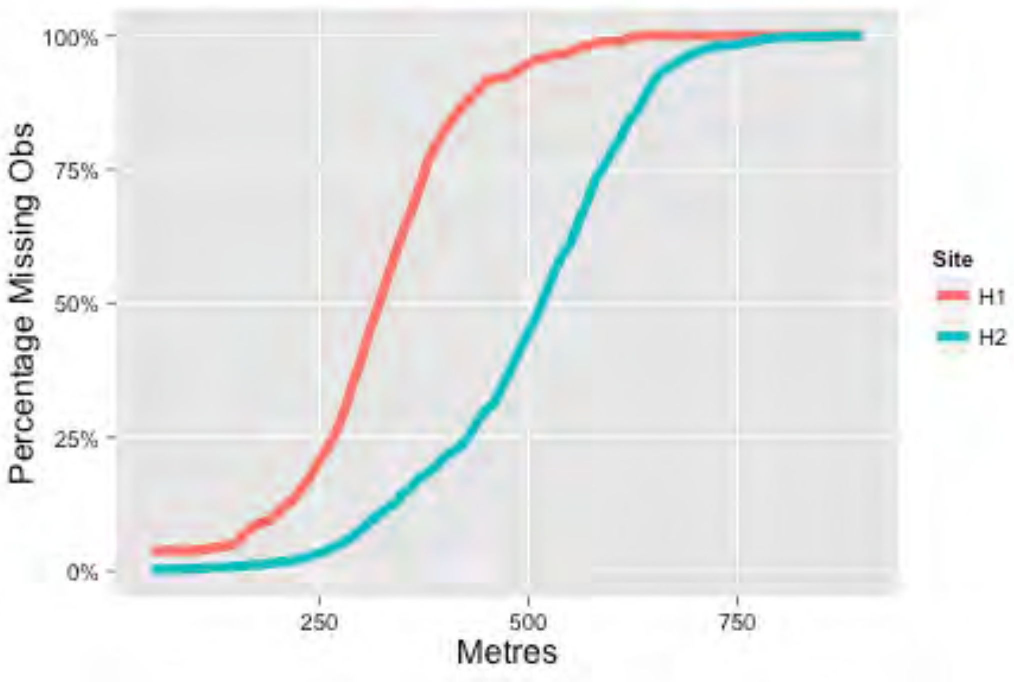

Figure 5-1. Percentage of missing RSS temperature observations by elevation above H1 and H2: 12pm to 6pm

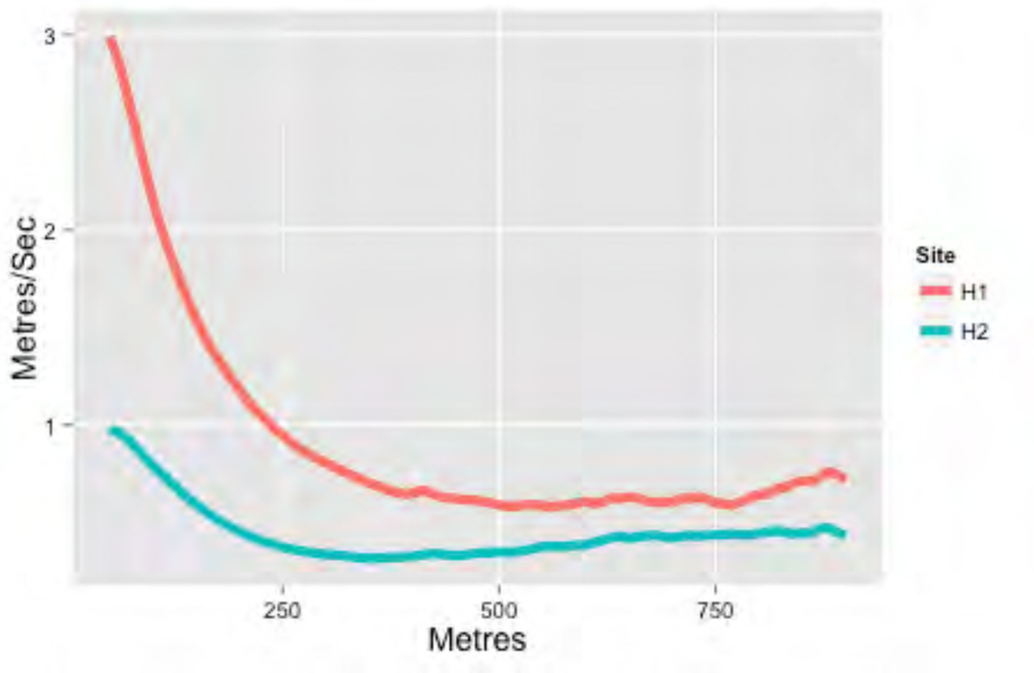

Figure 5-2. Average vertical wind speeds above H1 and H2: 12pm to 6pm

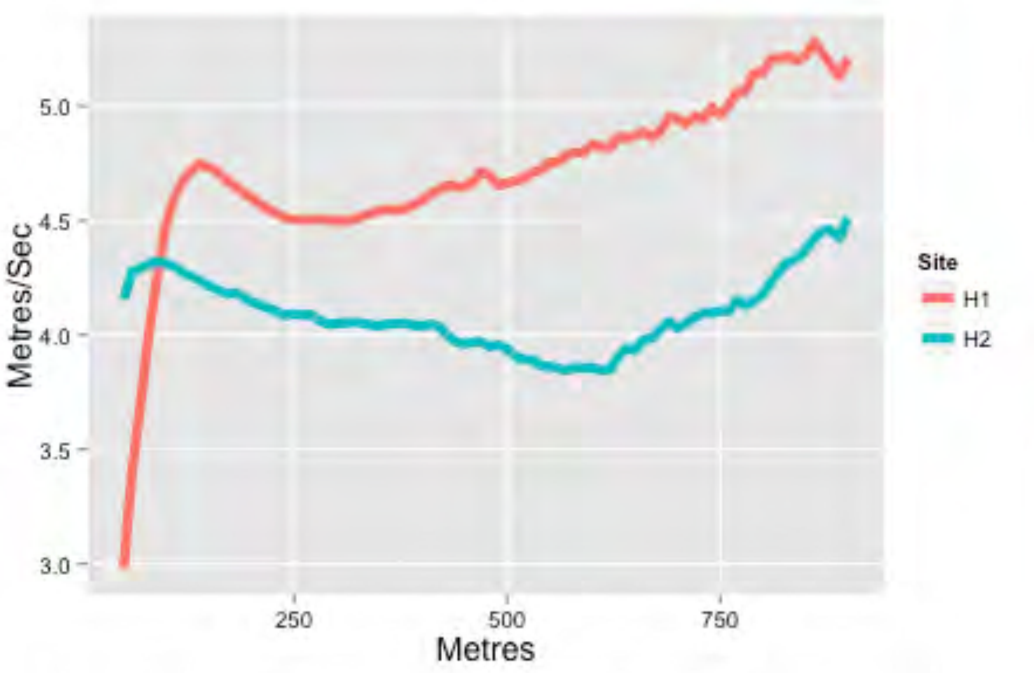

Figure 5-3. Average horizontal wind speeds above H1 and H2: 12pm to 6pm

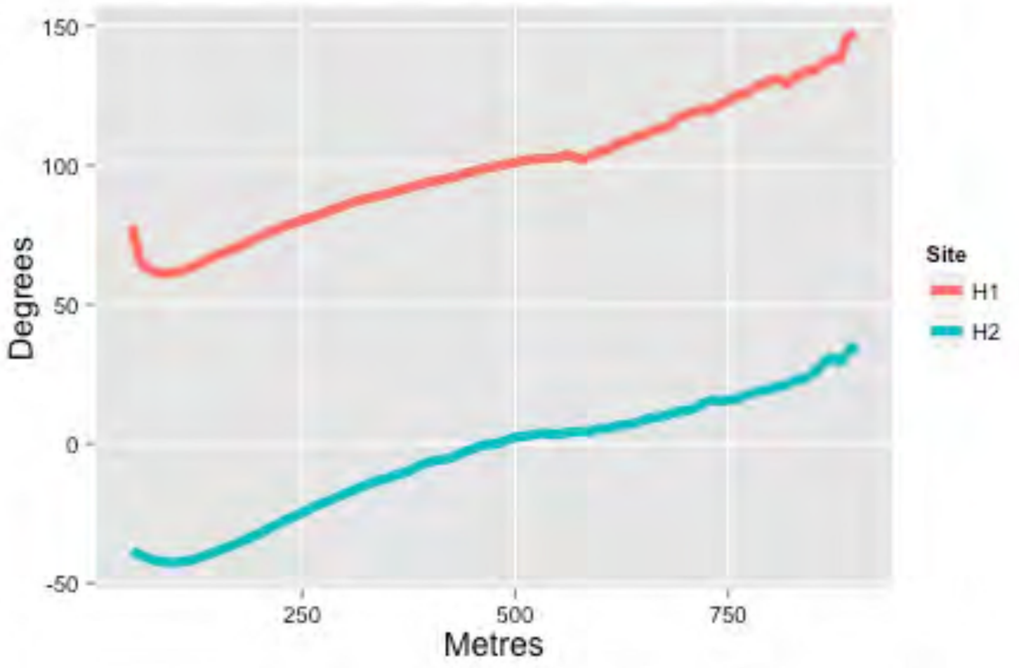

Figure 5-4. Speed weighted average wind directions above H1 and H2: 12pm to 6pm

Average horizontal wind speeds and directions by height are shown for H1 and H2 in Figures 5-3 and 5-4. Carried at these speeds, an ion plume would drift laterally 1.2km at H1 and 4.8km at H2 before reaching the average boundary layer height. Again using the 90th percentile boundary height the lateral distance would increase to almost 2km at H1 and 6.3km at H1. On average, the plume would smoothly clock about 100 degrees, from northeast to southeast at H1 and from northwest to northeast at H2.

In summary, vertical uplift on an ion plume is relatively short and the lateral orographic influences on an ion plume are small in relation to the size of the target area. As a consequence the downwind area (the footprint) should essential be determined by the direction and speed of upper winds in the free atmosphere. However, there is a relevant difference in the shape of a corridor model that extends laterally from the site perpendicular to the upper wind direction and a wedge that extends radially from the site. Lateral movement of the ion plume due to orographic influences would generally not alter the classification of gauges as targets or controls with the corridor model. With a wedge, these lateral movements may lead to quite different sets of target and control gauges near a site. One additional concern is that lateral flows due to orographic effects at H2 are larger and in the direction of H4, which would increase the potential for the control area at H3 to be exposed when H2 is active. Misclassifying an exposed gauge as a control would not lead to a positive overstatement of exposure to the ion plume, as it would simply tend to diminish the difference between any positive affect in the target area and what was recorded in the control area. However, it does make a signal more difficult to detect.

5.2. Upper air wind flows

There are two issues with the upper level radiosonde released from Seeb airport. The first is the selection of a relevant pressure interval. The second is that the Bureau of Meteorology releases only one radiosonde at 3am each morning.

5.2.1. Elevation of free atmospheric wind flows

Atmospheric pressures at Seeb of 500hPa and 700hPa correspond to elevations in the range of 3,000 to 5,600 metres. Atmospheric pressures between 700hPa and 850hPa correspond to elevations in the range of 1,500 to 3,000 metres, roughly in line with the peaks of the Hajar Mountains.

As can be seen in the plot of daily average wind directions (Figure 4.6), Seeb winds between 500hPa and 700hPa are quite consistent, with 80 per cent of the wind out of the three north to east quadrants. Seeb winds between 700hPa and 850hPa are from the west to northeast quadrants with 80 per cent of the wind out of these five quadrants. This shift in wind directions is similar to what is observed at H2, with the predominant wind direction being from the north, suggesting a similar orographic influence, as the orographic effects of the Hajar ranges on the height of the boundary layer can be expected to be felt well in advance of the ranges themselves.

It appears that winds at 700hPa to 850hPa above Seeb are therefore still within the boundary layer. Those between 500hPa to 700hPa are most likely to be in the free atmosphere, as their range extends well above of the estimated heights of the boundary layer at H1 and at H2. As a consequence, using the Seeb winds between 500hPa and 700hPA to define the ATLANT™ footprint seem appropriate.

5.2.2. Timing of the radiosonde

The 4am Seeb radiosonde is nine or more hours prior to the time that convective clouds begin to form over the Hajar Mountains. While free atmospheric wind flows are not diurnal substantive wind shifts may still occur over this period if high and low pressure cells move through the region. To gain some appreciation of the extent to which upper level winds shift over the day, daily changes in wind direction were calculated on a continuous scale.[1] These

[1] Where the absolute value of the difference exceeded 180 degrees, it was reflected back in the opposite direction to create a continuous scale. So a change of 270 degrees would become -90 and a change of -270 degrees would become +90.

differences were then halved to approximate a 4am to 4pm change and are shown in Figure 5.5.

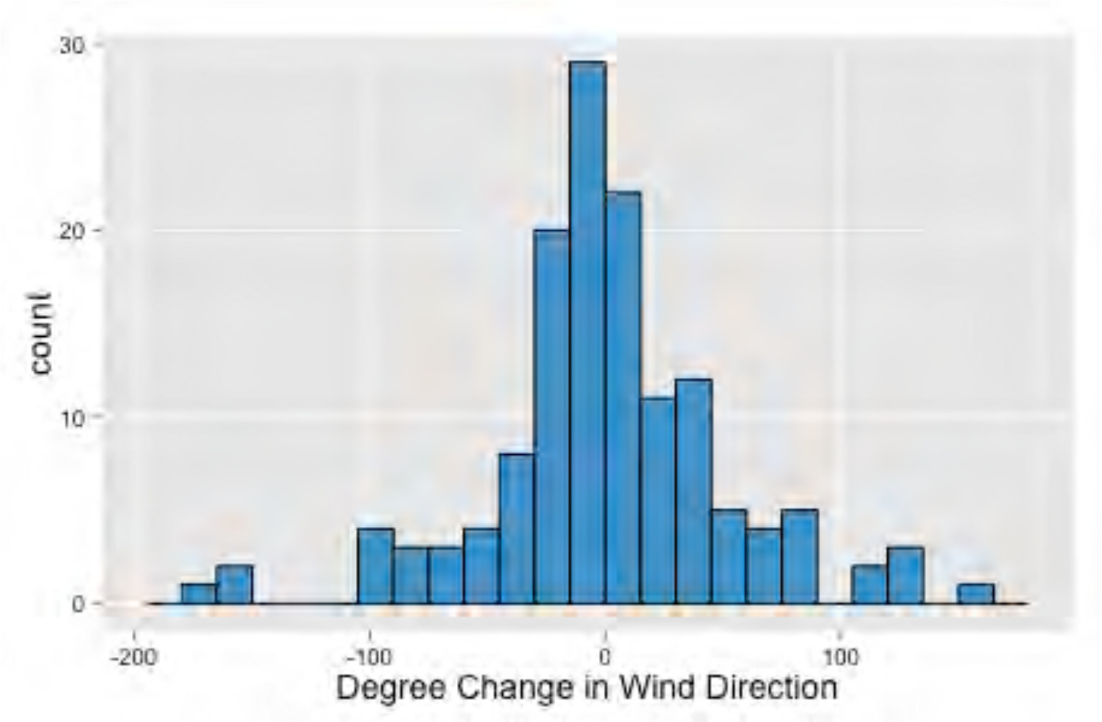

Figure 5.5. Approximate distribution of 4am to 4pm changes in 500hPa to 700hPa wind directions above Seeb airport.

Roughly 50 per cent of the changes are within 45 degrees of zero and more than 60 per cent are within 60 degrees. These may be captured within a reasonably broad corridor footprint. However, they would have a substantial impact on gauge classification near a site with a radially defined wedge footprint. , There are substantial number of larger changes, about 20 per cert of the changes exceed 60 degrees and include a limited number of wind reversals that would impact on gauge classification of any useful footprint.

It is possible to average the current and next day morning radiosonde readings to try for a better approximation of the afternoon wind directions. This clearly depends on the assumption that the transition in wind direction is reasonably slow and smooth. However, when high and low pressure systems move directly through the region, changes in wind direction are often large and abrupt. The only way to really resolve this issue is to conduct more timely radiosonde measurements.

5.3. Design Balance

Overall a corridor model appears to the most stable with respect wind direction and the classification of target and control gauges. Regardless of how the footprint is defined, it highly desirable that it generates a balanced sample of target and control gauges. While the experimental design for operation of the ATLANT^{TM} s is balanced, the short length of the trial and variability in wind directions will lead to some degree of imbalance in target and control gauges.

Given the operating schedule of the trial, Seeb 500hPa to 700hPa wind directions were used to set a corridor around each of the ATLANT^{TM} sites. The corridor is 30km wide perpendicular to the direction of the wind and 75km long parallel to the direction of the wind. A gauge is classified as a target if it lies within the downwind corridor when a site is in operation. A gauge is classified as a control if it lies within the downwind corridor of an inactive site, and does not lie within the downwind corridor of any active ATLANT^{TM} site.

The overall balance between target and control gauges is shown in the bubble plots in Figure 5-7. In the plots, the area of the bubble indicates the proportion of the time a gauge is either a target (top part of the figure) or a control (bottom part of the figure). The colour of the bubble reflects the number of days that rainfall was recorded at that gauge.

The balance appears to be quite good. This can be attributed to the relative consistency in upper level wind directions over the trial and the propensity for localised rain events that occur over the trial area to be spread fairly evenly over it.

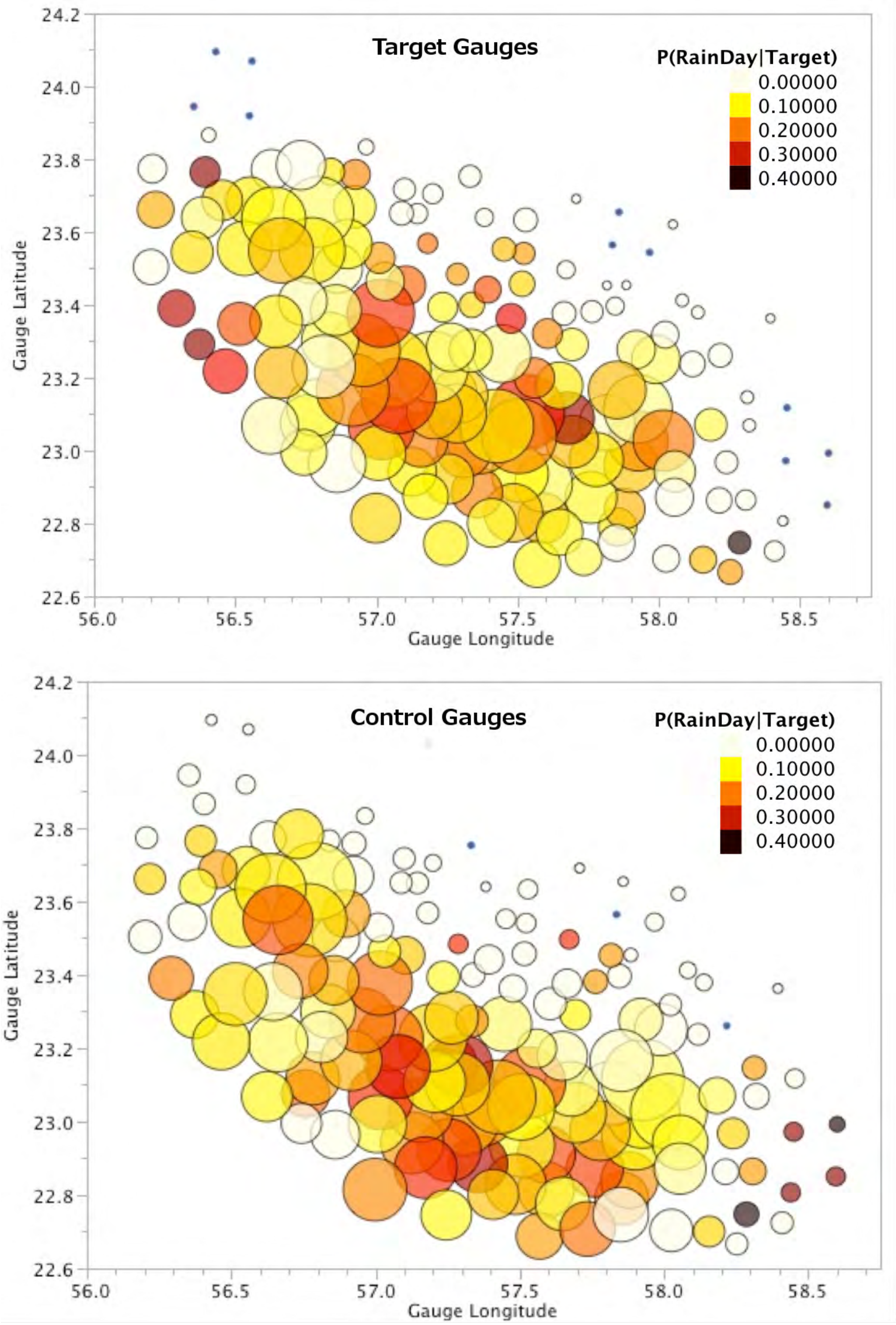

Figure 5-7. The proportion of times gauges served as a target or control (bubble area) and the proportion of rain days recorded at each gauge (bubble colour)

6. STATISTICAL MODELS

The statistical models used to identify and measure whether the ATLANT^{TM} systems have generated a rainfall enhancement signal over the course the trial are presented in this section. Four models were estimated, based on:

- Data from H1 and H2 with a dynamic downwind/upwind corridor
- Data from H1 and H2 with a dynamic downwind/upwind wedge
- Data from H1, H2, H3 and H4 with a dynamic downwind/upwind corridor
- Combined 2013 and 2014 data from H1 and H2 with a dynamic downwind/upwind corridor

The first two models are intended to provide estimates that are comparable to the data and methodology used in 2013. The remaining models are also based on the 2013 methodology. In keeping with the use of the 2013 methodology, the time window for the 2014 analysis was extended two hours prior to and after the period when summer convective cloud formation occurs over the Hajar Mountains; i.e. from 10am to 8pm. This was done to account lead and lag times that could be expected with respect to the downwind transport of the ion plume

The dynamic footprints are all defined with respect to Seeb 500hPa to 700hPa wind directions and centred at the ATLANT^{TM} sites. Again, footprint corridors are 30km wide in the direction perpendicular to the daily wind direction and extend 75km along the daily wind direction. The footprint wedges have an internal angle of 60 degrees at the ATLANT^{TM} site and contain gauges that are no more that 75km from the site.

6.1. Modelling Approach

Detecting a relatively small signal in a highly variable natural environment is a difficult task. Randomised experimental designs can offer a degree of control and eliminate experimental bias. However, statistical models are essential tools for controlling natural variably and increasing the signal to noise ratio of any ATLANT^{TM} signal given it exists.

Efficiency and bias are two critical elements of statistical modelling. Efficiency in this case relates to the precision of estimation of the natural rainfall that would have occurred at a target rainfall gauge if the ATLANTTM system(s) were not in operation. Bias is the concern that the modelling will undermine the experimental design, thus overstating the signal and the level of confidence in that signal.

Efficiency depends on having as much independent covariation between the variable to be explained, i.e. rainfall, and the covariates used to explain it. The use of gauge level rainfall observations has the greatest potential for efficiency but can introduce bias with respect to precision with respect to the estimates of natural rainfall that are made, due to spatiotemporal correlation in gauge observations. The analysis of spatial and temporal correlation in rainfall observations presented in Section 4 suggests that this may not be a large problem but it should not be ignored.

Correlation in rainfall observations may be accounted for, in part, by the use of spatial covariates such as gauge elevation and temporal covariates such as weather conditions. However, correlations that persist are reflected in the model prediction errors and can lead to an overstatement of the precision with which natural rainfall is estimated. Correcting for this bias is possible, but it is complex and achieved though numerical approximation techniques discussed later.

The selection of model covariates also presents issues of bias and efficiency. There are two principal sources of bias. The first is existence of relevant meteorological and spatial covariates that are not included in the model but are correlated with covariates that are in the model. The relevant excluded effect is, in part, transferred to the included covariates, imparting either a negative or a positive bias to the effect being measured. A statistical model of a natural system is generally open to omitted variable bias. One way in which such a bias could arise is discussed below.

The locations of the gauges that corresponding to targets and controls within a day are different and will be influenced by different orographic conditions, leading perhaps to one group to recording higher levels of natural rainfall than the other. Over a very long period of time this will not matter, as the randomised crossover experimental design will cancel out this difference, gauges tending to be targets and controls in equal proportion under similar conditions. However, given the relatively short length of the ATLANT^{TM} trial and natural variability in rainfall it is quite possible that it would have naturally rained more on the days that one of the groups served as a control. If this higher rainfall was due all or in part to some unmeasured meteorological covariate this would create an omitted variable bias.

The approach taken here to limit this problem is to introduce random effects for the different trial days to sweep out unaccounted-for metrological influences in the ATLANT^{TM} footprint on any given day. Effectively, average difference in rainfall from day to day is removed and only location specific differences within a day are retained. Random gauge effects can also be introduced to sweep out the variation in average gauge reading in different locations for much the same reason. Here, the objective is to sweep out unmeasured differences in the topography at different locations that may impact on rainfall, by taking out the variation in gauge level averages that may lead to an unobserved imbalance in the target and control gauges.

A second source of bias arises when predicting natural rainfall is using rainfall data that may contain an enhancement signal. The meteorological covariates will absorb all or part of the enhancement signal as the level of enhancement and natural rainfall are dependent on the same conditions. This problem is addressed through the use of an instrumental rainfall variable. This variable is estimated by first constructing a model that predicts rainfall using only gauge level data from those gauges that are not exposed to an ion plume generated by the ATLANT^{TM} system on the day, i.e. upwind gauges. The model includes gauge elevations as well as meteorological covariates, which are then used to predict downwind natural rainfall. This predicted value is referred to as the instrumental variable in what follows.

6.1.1. Rainfall Data

Statistical rainfall modelling is generally done using a two-step process, as the data is mixture of continuously distributed positive observations and a discrete probability mass at zero corresponding to days of no rainfall. Failing to account for the mix of continuous and discrete data is a third source of bias.

In the first stage the probability of observing a positive observation is calculated. This can be done using a suitable statistical model for a binary variable (e.g. a logistic model). But the proportion of positive observations in the sample is also an estimate. This ignores the possibility that the ion plume may increase the probability of observing a rainfall event. However, previous studies have failed to indicate any link between operation of the ATLANT™ system and propensity for rainfall to occur.

In the second stage, the positive rainfall observations are then modelled to predict rainfall levels given a rainfall event has occurred. These are the models presented here, from which conditional estimates of natural and enhanced levels of rainfall are derived. Unconditional estimates can be obtained by multiplying the volume of rain given a rainfall event occurred by the probability of the rainfall event.

Prior to modelling, positive rainfall observations are converted to a log scale. This has been done because the distribution of rainfall is quite asymmetric; possessing a very long right hand tail, as can be seen in Figure 6-1.

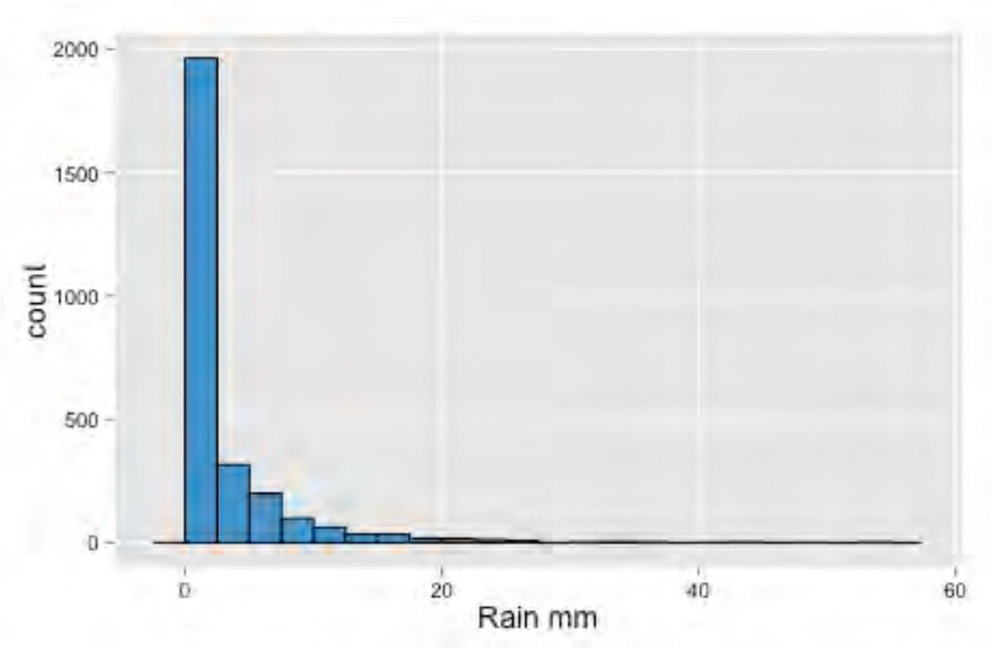

Figure 6-1. Positive TIE rainfall gauge observations: Jun1 to 18 October

6.2. Upwind Models

The upwind models are used to make out-of-sample predictions of downwind gauge rainfall from upwind gauge data. There are a number of possible meteorological covariates to choose from, as explored in Section 4. While there is no reason to impose a specific structure on the upwind model, there is a need for structural stability - that is, having model coefficients that are estimated with a reasonable high degree of precision. To this end:

- Principal component (PC) transformations were used in order to remove the spatial correlation between meteorological measurements from the DGMAN weather stations;
- Selection of models were through an automated stepwise regression procedure.

Trial day and gauge random effects were tested in each model and retained if significant.

The models were specified for gauges upwind of H1 and H2. The upwind corridor model is presented in Table 6-1. The upwind corridors are the mirror image of the downwind corridors reflected 180 degrees to the steering wind (see previous figure 1-2).

Table 6-1. Upwind H1–H2 corridor model

R-Square = 0.451				
Observations = 163				
Fixed Effect	Estimate	Std. Error	t-ratio	Sig. Level
Intercept	-0.8364	0.2441	-3.43	0.001
Gauge Elevation	0.0009	0.0003	3.36	0.001
Dry Temp PC2	0.4761	0.1652	2.88	0.007
Dew Point PC1	0.2149	0.0801	2.68	0.011
Random Effect	Ratio	Component	Std. Error	Variation %
Trial Day	0.2060	0.3036	0.1793	17.08
Residual		1.4737	0.1815	82.92

Table 6-2. Upwind H1–H2 wedge model

R-Square = 0.457				
Observations = 367				
Fixed Effect	Estimate	Std. Error	t-ratio	Sig. Level
Intercept	26.6836	10.4983	2.54	0.013
Gauge Elevation	-0.4680	0.1824	-2.57	0.013
Dry Temp PC2	0.4297	0.0986	4.36	0.000
Dew Point PC1	0.3201	0.1616	6.87	0.000
Random Effect	Ratio	Component	Std. Error	Variation %
Trial Day	0.1744	0.2839	0.1274	14.50
Gauge	0.0279	0.0453	0.0790	2.32
Residual		1.6277	0.1316	83.18

6.3. Downwind Models

The downwind models are more structured than the upwind models as they are specifically designed to detect an ATLANT[TM] signal based on the designation of a gauge as a target or a control. There are different possible specifications based on factors that take on a value of either zero or one, including:

- A designation of a gauge as either a target or control that is regardless of which site is currently a target or control (not site specific);
- A designation of gauge as either a target or control is in specific relation to a site;
- An interaction between a gauge designation and another model covariate.

The first two specifications allow a simple test of generic overall effect versus a site-specific effect. It should be noted that in both cases, a control gauge is an implicit designation. Predicted rainfall at a control gauge is determined by the remaining model parameters, including a constant term and random effects.

The balance of the model covariates were again selected using a stepwise regression procedure. Models initially included a gauge day and gauge random effects, but only significant random effects were retained.

6.3.1. The 2014 H1 and H2 Models

Models were estimated using only gauges downwind of H1 and H2 in 2014 to allow direct comparisons to be made with the results from the 2013 trial. There were two general differences between the 2013 and 2014 specifications. First, there were additional covariates available from the SODAR data in 2014. Second, the target by elevations interactions, which were significant in 2013, were not significant in 2014. This is discussed are the end of this section.

Four models were estimated:

- A corridor model with a generic target designation;
- A corridor model with a site specific designation;
- A wedge model with a generic target designation;
- A wedge model with a site specific target designation.

The results are summarised in Tables 6-3 though 6-6. In general the instrumental prediction of downwind rain generated from the corresponding upwind model is highly significant in all of the models. The dominant SODAR zone and meridian wind values at H1 and H2 are also significant. Gauge elevation is significant in the corridor models but not in the wedge models. The wedge model contains a larger proportion of gauges at lower elevations and the higher level gauges have greater variability in gauge elevation. Average target and control gauge elevations were about 100 metres lower in the wedge as opposed to the corridor model.

The corridor model has a significant non site-specific target effect. As with 2013, it was not possible to isolate clearly significant site-specific effects at both H1 and H2. However, there is a significant effect at H2 at the 90 per cent confidence level and marginally significant effect at H1 at the 87 per cent confidence level.

In contrast to the 2013 model, the interaction between target gauge designations and elevation were not significant in the 2014 models.

Table 6-3. Results for the 2014 H1 and H2 corridor model with a non site-specific target designation

R-Square = 0.248				
Observations = 479				
Fixed Effect	Estimate	Std. Error	t-ratio	Sig. Level
Intercept	0.7952	0.2092	3.80	0.000
Gauge Elevation	-0.0001	0.0002	-3.50	0.001
Instrumental Rain	0.7597	0.1474	5.15	0.000
H1 SODAR Zone	-0.1728	0.0577	-2.99	0.004
H2 SODAR Meridian	0.1854	0.0688	2.69	0.009
Combined H1 H2 Target	0.2676	0.1268	2.11	0.035
Random Effect	Ratio	Component	Std. Error	Variation %
Trial Day	0.1242	0.2181	0.1008	11.05
Residual		1.7555	0.1259	88.95

Table 6-4. Results for the 2014 H1/H2 corridor model - site-specific target designations

R-Square = 0.248				
Observations = 479				
Fixed Effect	Estimate	Std. Error	t-ratio	Sig. Level
Intercept	0.7940	0.2103	3.78	0.000
Gauge Elevation	-0.0007	0.0002	-3.45	0.001
Instrumental Rain	0.7598	0.1488	5.11	0.000
H1 SODAR Zone	-0.1725	0.0579	-2.98	0.004
H2 SODAR Meridian	0.1856	0.0693	2.68	0.009
H1 Target	0.2695	0.1756	1.53	0.126
H2 Target	0.2657	0.1573	1.69	0.092
Random Effect	Ratio	Component	Std. Error	Variation %
Trial Day	0.1260	0.2214	0.1029	11.19
Residual		1.1577	0.1264	88.81

Table 6-5. Results for the 2014 H1/H2 wedge model - non site-specific target designation

R-Square = 0.272 Observations = 461				
Fixed Effect	Estimate	Std. Error	t-ratio	Sig. Level
Intercept	0.1007	0.1882	0.53	0.593
Gauge Elevation	8.7e-7	0.0001	0.01	0.996
Instrumental Rain	0.7258	0.119	6.06	0.000
H1 SODAR Zone	-0.1404	0.0597	-2.35	0.022
H2 SODAR Meridian	0.1861	0.0694	2.68	0.009
Combined H1 H2 Target	0.2210	0.1325	1.67	0.096
Random Effect	Ratio	Component	Std. Error	Variation %
Trial Day	0.1178	0.2108	0.0990	10.54
Residual		1.7904	0.1301	89.46

The results for the wedge model are similar, though this model does not yield an ATLANT^{TM} signal that is as clear as that generated by the corridor model. This was also the case in the 2013 trial. There is a significant non site-specific ATLANT^{TM} effect at the 90 per cent confidence level. There are no significant site-specific effects, although the H2 effect is almost significant at this level as well.

Table 6-6. Results for the 2014 H1 and H2 wedge model with site-specific target designations

R-Square = 269				
Observations = 479				
Fixed Effect	Estimate	Std. Error	t-ratio	Sig. Level
Intercept	0.1018	0.1880	0.54	0.587
Gauge Elevation	8.8e-7	0.0002	-0.05	0.959
Instrumental Rain	0.7342	0.1204	6.1	0.000
H1 SODAR Zone	-0.1386	0.0595	-2.33	0.023
H2 SODAR Meridian	0.1830	0.0694	2.64	0.011
H1 Target	0.1667	0.1843	0.9	0.366
H2 Target	0.2607	0.1617	1.61	0.108
Random Effect	Ratio	Component	Std. Error	Variation %
Trial Day	0.1137	0.2043	0.1011	10.21
Residual		1.7974	0.1313	89.79

6.3.2. The 2014 Full Trial Model

The estimates for the full set of trial observations at H1 through H4 were done using the corridor model. As a non site-specific effect was established at H1 and H2, the full model is only specified with site-specific target gauge designations. The instrumental predictions of downwind rain are based on the H1 H2 upwind corridor model. They are again, highly significant as is gauge elevation. The dominant zone and meridian wind values at H1 and H2 are also significant.

The target designations at H1, H2 and H3 are significant. The significance of the effects at H1 and H2 may be attributed to the larger data set and the greater precision with which the coefficients of the other model covariates have been estimated. The larger and highly significant effect at H3 may to some extent be due to the greater levels of rainfall observed in the northwestern part of the trial area. There was no significant effect at H4 in the southeastern end of the trial area.

Table 6-7. Results for the 2014 H1 through H4 corridor model with site-specific target designations

R-Square = 227				
Observations = 807				
Fixed Effect	Estimate	Std. Error	t-ratio	Sig. Level
Intercept	0.7638	0.1610	4.74	0.000
Gauge Elevation	-0.0007	0.0002	-4.35	0.000
Instrumental Rain	0.8680	0.1108	7.83	0.000
H1 SODAR Zone	-0.0992	0.0452	-2.20	0.032
H2 SODAR Meridian	0.1175	0.0538	2.18	0.034
H1 Target	0.3046	0.1669	1.83	0.068
H2 Target	0.3049	0.1459	2.09	0.037
H3 Target	0.5517	0.1751	3.15	0.002
H4 Target	-0.1731	0.1768	-0.98	0.328
Random Effect	Ratio	Component	Std. Error	Variation %
Trial Day	0.0741	0.1377	0.0626	6.90
Residual		1.8595	0.0988	93.10

6.3.3. The combined 2013 2014 Trial Model

At H1 and H2 it was possible to combine the 2013 and 2014 trial data. Upwind estimates of the model used to generate instrumental predictions of downwind rainfall were made using the upwind corridor model discussed earlier, using data from both years. The downwind model makes use of the corridor model used in 2013, which includes site specific target designations and target elevation interactions. The data loggers at the H1 and H2 weather station failed in 2014 so it was not possible to include the humidity and radiation covariates that were used in 2013.

The results are summarised in Table 6-8. In general the 2013 and the combined 2013/14 model are quite similar. While the presence of interactions in the model specification makes it difficult to ascertain the significance of the site-specific effects, there is a substantial increase in the precision of the target and target elevation interactions in the combined model. The relative size of the target versus the target by elevation parameters is indicative of:

- A highly significant attribution at H1
- A significant attribution at H2

Table 6-8. Results for the combined 2013 and 2014 trials at H1 and H2: corridor model with site-specific gauge designations

R-Square = 0.264				
Observations = 946				
Fixed Effect	Estimate	Std. Error	t-ratio	Sig. Level
Intercept	0.3679	0.1464	2.51	0.012
Gauge Elevation	0.0000	0.0001	0.28	0.778
Instrumental Rain	0.7025	0.1101	6.38	0.000
H1 Target	0.5621	0.2320	2.42	0.016
H2 Target	0.3280	0.2192	1.5	0.135
Elevation by H1 Target	-0.0005	0.0002	-1.97	0.050
Elevation by H2 Target	-0.0004	0.0002	-1.73	0.083
Random Effect	Ratio	Component	Std. Error	Variation %
Trial Day	0.1812	0.3263	0.0813	15.3
Residual		1.8004	0.0908	84.4

6.3.4. Gauge elevations in the 2013 and 2014 trials

The balance of H1 and H2 target and control gauge elevations in in the 2013 and 2014 trials is worth investigating, given:

- Gauge elevation was a significant covariate in the corridor model but not the wedge model in 2013 and 2014
- The target by elevation interaction terms were significant in the corridor and wedge models in 2013 but not in 2104.
- The target by elevation interaction term were more significant in the combined 2013 2014 corridor model than in 2013 corridor model.

The average target and control elevations at H1 and H2 for the corridor model are shown in Table 6-9. The average elevations under the wedge model are clearly lower than the corridor model in both years. The wedge model does tend to limit the number of high elevation gauges near the H1 and H2 sites.

While there are substantial differences in target and control gauge elevations within and between years, there are no clear patterns that suggest an explanation for why the target by elevation interaction terms were significant in one year and not the next.

A more detailed exploration of the spatial distribution of gauge locations may be warranted from a model diagnostic point of view and for the future selection of gauge locations. However, with repeated trials these concerns should be resolved through the experimental design and the greater flexibility in model specification that a large number of observations should provide.

Table 6-9. Average target and control gauge elevations at H1 and H2 in 2013 and 2014, on days when at least one gauge recorded rainfall

Site/Model	2013		2014	
	Target	Control	Target	Control
Corridor Model				
H1	920	862	762	819
H2	836	915	956	897
Wedge Model				
H1	777	627	638	708
H2	732	799	812	735

7. THE ESTIMATED RAINFALL ENHANCEMENT EFFECT

The attribution estimates for each of the four models are presented in the section. First the methodology for calculating the attributions is explained. This is followed by the ATLANT™ attributions.

7.1. Methodology

All of the downwind statistical models allow for two counterfactual simulations:

- How much natural rainfall would have been reported by target gauges if the ATLANT™ system had not actually operated?
- How much more rain would have been reported by control gauges if the ATLANT™ system had actually operated?

This is done simply by switching target gauges to the status of controls and comparing the difference in rainfall predicted by the model. The same switch and comparison can be made for control gauges. For the purpose of estimating an ATLANT™ attribution the target gauges are switched to control gauges. The enhancement effect is then calculated by subtracting the estimated amount of rain that would have been reported in this case (the natural rainfall) from the actual rainfall that was recorded. In order to calculate how much additional rain might have fallen if the ATLANT™ system had been continuously operated at each site both counterfactuals are required.

The ATLANT™ attribution is expressed as the ratio of the estimated difference in rainfall attributed to ATLANT™ divided by the estimate of natural rainfall. Estimating the confidence one can have in this ratio presents a problem. There is joint uncertainty in the numerator (attribution) and the denominator (natural rainfall), which are not independent, as generally a higher attribution would be expected with higher levels of natural rainfall. This is a reflection of the sampling errors associated with the coefficients of the model used to estimate the natural rainfall, which are themselves a function of the model errors and the correlations between the covariates.

The way to deal with this problem is though numerical approximation. The attribution ratio can be repeatedly calculated by drawing random samples of the coefficients of this model from their joint sampling distribution. This enables an empirical estimate of the sampling distribution of the attribution ratio to be obtained, and consequently allows the mean and confidence bounds for this ratio to be ascertained.

This would be relatively straight forward if the model errors were independent, as the sampling distribution of the estimates of the model coefficients are then essentially defined by the model variance covariance matrix. However, it must be assumed that these errors are correlated in time, space or combinations of space and time, and the so the sampling distribution of the estimates of the model coefficients is unknown. In such a case it becomes necessary to rely on another form of numerical approximation to estimate the sampling distribution of the model coefficients. This technique is known as resampling, and the most common method of implementing it is referred to as a bootstrap.

The basic idea behind the bootstrap is to resample the data and consequently re-estimate the model coefficients a sufficient number of time in order to construct an empirical estimate of their sampling distribution. The key here is to resample the data in way that preserves the spatiotemporal correlation. This is implemented by classifying the data to blocks that are nearby in space and time, and then resampling from these blocks rather than from the data set as a whole. If the data within the blocks are correlated this method will ensure that this correlation is preserved, and is appropriately reflected in the samples that are drawn. In our case the blocks are defined by both day and by downwind corridor. Gauges within a block are therefore nearby in a spatial sense but also change daily in line with the change in the wind direction that defines the downwind corridor. Hence the term for the technique, spatiotemporal block bootstrap.

7.2. ATLANT™ Attributions

All of the models that were presented in the previous section generate significant ATLANT™ attributions. The results presented here are for the site-specific target and control gauge designations. The models estimated using data from only H1 and H2 give very similar results to those obtained in 2013. The enhancement effect for the corridor model is 18 per cent with a confidence level of 99 per cent in 2013 and an enhancement effect of 21.7 per cent and confidence level of over 99 per cent in 2014. The corresponding figure for the wedge model is an enhancement effect of 11.7 per cent with a confidence level of 90 per cent in 2103 and an enhancement effect of 16.3 per cent and a confidence level of over 95 per cent in 2014.

The data for the full 2014 trial gave a very large estimate of the enhancement effect of almost 33 per cent with a lower 90 per confidence bound greater than the mean effect of any of the other models. This was despite having an insignificant but negative effect at H4. However, there are reasons to be circumspect about this result. First, the highest and most variable rainfall fell in the area around H3 in the northwest. The experimental design and model covariates provide only a partial degree of control for the natural variability in rainfall. With higher levels of natural variability there is simply a greater potential for substantially larger volume of rainfall to fall in either target or control gauges over the length of a short trial. Second, the potential number of gauges in the downwind vicinity of H3 and H4 is lower as these sites are at the edges of the trial area. Additional trials with an expended gauge network seem likely to temper the 2014 full trial results.

The estimates obtained by combining H1 and H2 data from 2013 and 2014 provided consistent data set over a longer time horizon, which allows greater control through the experiment design and greater variation in the model covariates. As such, these estimates may be the most reliable ATLANT™ attribution results obtained to date. The combined data set yielded an enhancement effect of 18.5 per cent and a confidence level of over 99 per cent. Table 7-1 provides a summary of these modelling results. Note that these values are based on the spatio-temporal block bootstrap distributions that were generated for each footprint definition.

Table 7-1. Summary of model results

Footprint/Variable	10th	50th	90th	Mean	Std. Error	Sig. Level
H1 H2 Corridor						
Total Rainfall mm	1,893	2.233	2,666	2,263	310	
Natural Rainfall mm	1,535	1,841	2,229	1,866	282	
Atlant Attribution mm	248	387	555	397	122	
Atlant Attribution %	12.8	21.2	221.2	21.7	7.3	0.003
H1 H2 Wedge						
Total Rainfall mm	1,723	2,063	2,516	2,103	348	
Natural Rainfall mm	1,462	1,769	2,196	1,808	318	
Atlant Attribution mm	156	282	446	298	119	
Atlant Attribution %	8.4	16.0	25.6	16.3	6.92	0.016
H1 – H4 Corridor						
Total Rainfall mm	3,175	3,698	4,345	3,734	465	
Natural Rainfall mm	2,348	2,780	3,341	2,819	394	
Atlant Attribution mm	672	903	1,169	915	196	
Atlant Attribution %	23.2	32.7	42.9	32.9	7.6	0.000
2013-14 Corridor						
Total Rainfall mm	3,978	4,567	5,296	4,606	517	
Natural Rainfall mm	3,307	3,852	4,549	3,897	489	
Atlant Attribution mm	460	695	975	709	202	
Atlant Attribution %	11.3	18.1	26.3	18.5	5.8	0.001

8. CONCLUDING COMMENTS

The results from the 2014 trial yielded relatively consistent and positive results that align closely with those obtained in the 2013 trial.

The expanded gauge network has provided a much better picture of the temporal and spatial viability of rainfall in the Hajar Mountains. Precipitation is highly localised on a daily basis but there may be a strong northwest to southeast pattern in total precipitation. The expanded gauge network appears to have increased the reliability of the estimates at H1 and H2 that are in the centre of the trial area. The continued expansion of the network should prove valuable especially given the localised nature of daily rainfall

The additional instrumentation of the trial, SODAR and RSS at H1 and H2, provided a better understanding of the orographic features of the trial area and informed the choice of the downwind footprint that is critical to the statistical analysis of the trials.

The most significant improvement in the instrumentation of future trials is obtaining afternoon radiosonde measurements to track the flow of upper winds during the time convective clouds form over the Hajar Mountains. This would give us a more precise idea of downwind track of an ion plume after it entered the free atmosphere and the direction and extent of the downwind footprint.

9. REFERENCES

Al-Brashdl, Hamid Ahmed Sulaiman. 2007: Forecasting Techniques for seedable storms over the Western Hajar mountains in the Sultanate of Oman. MSc thesis. University of Pretoria.

Al-Maskari, J. and A. Gadian: 2001. A study of orographic convection over the Hajar Mountains in northern Oman. Presented at International Symposium on Nowcasting and Very Short Range Forecasting (WSN05).

Beare, S., R. Chambers, S. Peak, Statistical Modeling of Rainfall Enhancement. Journal of Wea. Modif. 42, 13-32, 2010.

Beare, S., R. Chambers, S. Peak, J. Ring,: Accounting for Spatiotemporal Variation of Rainfall Measurements when Evaluating Ground-Based Methods of Weather Modification. Journal of Wea. Modif. 43, 44-63, 2011.

Chambers, R., S. Beare, S. Peak (2012) Using Dynamically Defined Control Areas to Evaluate Impact of Cloud Ionization Technology. Journal of Wea. Modif. 44, 16-29.

Chambers, R. and Chandra, H. (2013). A random effect block bootstrap for clustered data. Journal of Computational and Graphical Statistics, 22, 452-470.

Chambers, R., S. Beare, S. Peak, Al-Kablani, M. (2015) Rainfall Enhancement in the Hajar Mountains, Oman, Journal of Wea. Modif. 45, submitted.

Charabi, Y. (2013) Projection of Future Changes in Rainfall and Temperature Patterns in Oman. J Earth Sci Clim Change 4:154.

FAO (2009) Groundwater Management in Oman. Draft Synthesis Report, Food and Agriculture Organization of the United Nations, Rome, 2009

Galway, J. G., 1956: The lifted index as a predictor of latent instability. Bull. Amer. Meteor. Soc., 528–529.

Miller, R. C., 1972: Notes on analysis and severe storm forecasting procedures of the Air Force Global Weather Central. Tech. Rept. 200(R), Headquarters, Air Weather Service, USAF, 190 pp.

APPENDIX A COMPLETED 2014 ATLANT™ OPERATION

Year	Month	Day	Exp. Day	H3	H1	H2	H4	Notes where planned operation not achieved
2014	6	1	1	Off	On	Off	On	
2014	6	2	2	On	Off	On	Off	
2014	6	3	3	Off	On	Off	On	
2014	6	4	4	On	Off	On	Off	
2014	6	5	5	Off	On	Off	On	
2014	6	6	6	Off	On	Off	On	
2014	6	7	7	On	Off	On	Off	
2014	6	8	8	On	Off	On	Off	
2014	6	9	9	On	Off	On	Off	
2014	6	10	10	Off	On	Off	On	
2014	6	11	11	Off	On	Off	On	
2014	6	12	12	Off	On	Off	On	
2014	6	13	13	On	Off	On	Off	
2014	6	14	14	On	Off	On	Off	
2014	6	15	15	On	Off	On	Off	
2014	6	16	16	Off	On	Off	On	The switching was reversed on 16/17 Jun. That is, where it says Off, it should have been On, and where it says On, it should have been Off
2014	6	17	17	On	Off	On	Off	
2014	6	18	18	On	Off	On	Off	
2014	6	19	19	On	Off	On	Off	
2014	6	20	20	Off	On	Off	On	
2014	6	21	21	On	Off	On	Off	
2014	6	22	22	Off	On	Off	On	
2014	6	23	23	Off	On	Off	On	
2014	6	24	24	Off	On	Off	On	
2014	6	25	25	Off	On	Off	On	
2014	6	26	26	On	Off	On	Off	
2014	6	27	27	Off	On	Off	On	
2014	6	28	28	On	Off	On	Off	
2014	6	29	29	Off	On	Off	On	
2014	6	30	30	Off	On	Off	On	
2014	7	1	31	Off	On	Off	On	
2014	7	2	32	On	Off	On	Off	

2014	7	3	33	On	Off	On	Off	
2014	7	4	34	Off	On	Off	On	
2014	7	5	35	On	Off	On	Off	
2014	7	6	36	Off	On	Off	On	
2014	7	7	37	Off	On	Off	On	
2014	7	8	38	Off	On	Off	On	
2014	7	9	39	On	Off	On	Off	
2014	7	10	40	On	Off	On	Off	
2014	7	11	41	On	Off	On	Off	
2014	7	12	42	On	Off	On	Off	
2014	7	13	43	Off	On	Off	On	
2014	7	14	44	On	Off	On	Off	
2014	7	15	45	Off	On	Off	On	
2014	7	16	46	On	Off	On	Off	
2014	7	17	47	Off	On	Off	On	
2014	7	18	48	On	Off	On	Off	
2014	7	19	49	On	Off	On	Off	
2014	7	20	50	On	Off	On	Off	
2014	7	21	51	On	Off	On	Off	
2014	7	22	52	Off	On	Off	On	
2014	7	23	53	On	Off	On	Off	
2014	7	24	54	Off	On	Off	On	
2014	7	25	55	Off	On	Off	On	
2014	7	26	56	Off	On	Off	On	
2014	7	27	57	On	Off	On	Off	
2014	7	28	58	Off	On	Off	On	
2014	7	29	59	On	Off	On	Off	
2014	7	30	60	Off	On	Off	On	
2014	7	31	61	Off	On	Off	On	
2014	8	1	62	Off	On	Off	On	
2014	8	2	63	On	Off	On	Off	
2014	8	3	64	Off	On	Off	On	
2014	8	4	65	Off	On	Off	On	
2014	8	5	66	On	Off	On	Off	
2014	8	6	67	Off	On	Off	On	
2014	8	7	68	On	Off	On	Off	
2014	8	8	69	On	Off	On	Off	
2014	8	9	70	On	Off	On	Off	
2014	8	10	71	Off	On	Off	On	
2014	8	11	72	On	Off	On	Off	
2014	8	12	73	On	Off	On	Off	
2014	8	13	74	Off	On	Off	On	

2014	8	14	75	Off	On	Off	On	
2014	8	15	76	On	Off	On	Off	
2014	8	16	77	Off	On	Off	On	
2014	8	17	78	On	Off	On	Off	
2014	8	18	79	On	Off	On	Off	
2014	8	19	80	Off	On	Off	On	
2014	8	20	81	Off	On	Off	Off	H4 was planned On, but actual operation was Off due to HVG cable failure
2014	8	21	82	On	Off	On	Off	
2014	8	22	83	Off	On	Off	Off	H4 was planned On, but actual operation was Off due to HVG cable failure
2014	8	23	84	On	Off	On	Off	
2014	8	24	85	Off	On	Off	Off	H4 was planned On, but actual operation was Off due to HVG cable failure
2014	8	25	86	On	Off	On	Off	
2014	8	26	87	On	Off	On	Off	
2014	8	27	88	On	Off	On	Off	
2014	8	28	89	On	Off	On	Off	
2014	8	29	90	Off	On	Off	Off	H4 was planned On, but actual operation was Off due to HVG cable failure
2014	8	30	91	Off	On	Off	Off	H4 was planned On, but actual operation was Off due to HVG cable failure
2014	8	31	92	On	Off	On	Off	
2014	9	1	93	Off	On	Off	Off	H4 was planned On, but actual operation was Off due to HVG cable failure
2014	9	2	94	Off	On	Off	Off	H4 was planned On, but actual operation was Off due to HVG cable failure
2014	9	3	95	Off	On	Off	Off	H4 was planned On, but actual operation was Off due to HVG cable failure
2014	9	4	96	On	Off	On	Off	
2014	9	5	97	Off	On	Off	Off	H4 was planned On, but actual operation was Off due to HVG cable failure
2014	9	6	98	On	Off	On	Off	
2014	9	7	99	Off	On	Off	Off	H4 was planned On, but actual operation was Off due to HVG cable failure

2014	9	8	100	Off	On	Off	On	
2014	9	9	101	On	Off	On	Off	
2014	9	10	102	Off	On	Off	On	
2014	9	11	103	On	Off	On	Off	
2014	9	12	104	Off	On	Off	On	
2014	9	13	105	On	Off	On	Off	
2014	9	14	106	Off	On	Off	On	
2014	9	15	107	On	Off	On	Off	
2014	9	16	108	Off	On	Off	On	
2014	9	17	109	On	Off	On	Off	
2014	9	18	110	On	Off	On	Off	
2014	9	19	111	Off	On	Off	On	
2014	9	20	112	On	Off	On	Off	
2014	9	21	113	On	Off	On	Off	
2014	9	22	114	Off	On	Off	On	
2014	9	23	115	Off	On	Off	On	
2014	9	24	116	Off	On	Off	On	
2014	9	25	117	On	Off	On	Off	
2014	9	26	118	On	Off	On	Off	
2014	9	27	119	On	Off	On	Off	
2014	9	28	120	Off	On	Off	On	
2014	9	29	121	On	Off	On	Off	
2014	9	30	122	On	Off	On	Off	
2014	10	1	123	On	Off	On	Off	
2014	10	2	124	Off	On	Off	On	
2014	10	3	125	Off	On	Off	On	
2014	10	4	126	Off	On	Off	On	
2014	10	5	127	Off	On	Off	On	
2014	10	6	128	On	Off	On	Off	
2014	10	7	129	Off	On	Off	On	
2014	10	8	130	On	Off	On	Off	
2014	10	9	131	On	Off	On	Off	
2014	10	10	132	Off	On	Off	On	
2014	10	11	133	Off	On	Off	On	
2014	10	12	134	On	Off	On	Off	
2014	10	13	135	Off	On	Off	On	
2014	10	14	136	On	Off	On	Off	
2014	10	15	137	Off	On	Off	On	
2014	10	16	138	Off	On	Off	On	
2014	10	17	139	On	Off	On	Off	
2014	10	18	140	On	Off	On	Off	